UPPSALA
UNIVERSITET

Digital Comprehensive Summaries of Uppsala Dissertations from the Faculty of Science and Technology 1160

Synthesis of Thin Piezoelectric AlN Films in View of Sensors and Telecom Applications

MILENA DE ALBUQUERQUE MOREIRA

ACTA
UNIVERSITATIS
UPSALIENSIS
UPPSALA
2014

ISSN 1651-6214
ISBN 978-91-554-8995-3
urn:nbn:se:uu:diva-229588

Dissertation presented at University of Campinas to be publicly examined in Conference Room, FEEC, UNICAMP, Av. Albert Einstein, 400 / Cidade Universitária Zeferino Vaz / Distrito Barão Geraldo, Campinas, Brazil, Wednesday, 24 September 2014 at 14:30 for the degree of Doctor of Philosophy. The dissertation can be followed via videolink at Beurlingrummet, Ångström Laboratory, Uppsala Universitet. The examination will be conducted in English. Faculty examiner: Dr. Ricardo Cotrin.

Abstract

Moreira, Milena De Albuquerque. 2014. Synthesis of Thin Piezoelectric AlN Films in View of Sensors and Telecom Applications. *Digital Comprehensive Summaries of Uppsala Dissertations from the Faculty of Science and Technology* 1160. 83 pp. Uppsala: Acta Universitatis Upsaliensis. ISBN 978-91-554-8995-3.

The requirements of the consumer market on high frequency devices have been more and more demanding over the last decades. Thus, a continuing enhancement of the devices' performance is required in order to meet these demands. In a macro view, changing the design of the device can result in an improvement of its performance. In a micro view, the physical properties of the device materials have a strong influence on its final performance. In the case of high frequency devices based on piezoelectric materials, a natural way to improve their performance is through the improvement of the properties of the piezoelectric layer. The piezoelectric material studied in this work is AlN, which is an outstanding material among other piezoelectric materials due to its unique combination of material properties.

This thesis presents results from experimental studies on the synthesis of AlN thin films in view of telecom, microelectronic and sensor applications. The main objective of the thesis is to custom design the functional properties of AlN to best suit these for the specific application in mind. This is achieved through careful control of the crystallographic structure and texture as well as film composition.

The piezoelectric properties of AlN films were enhanced by doping with Sc. Films with different Sc concentrations were fabricated and analyzed, and the coupling coefficient (k_t^2) was enhanced a factor of two by adding 15% of Sc to the AlN films. The enhancement of k_t^2 is of interest since it can contribute to a more relaxed design of high frequency devices. Further, in order to obtain better deposition control of c-axis tilted AlN films, a new experimental setup were proposed. When this novel setup was used, films with well-defined thicknesses and tilt uniformity were achieved. Films with such characteristics are very favorable to use in sensors based on electroacoustic devices operating in viscous media. Studies were also performed in order to obtain c-axis oriented AlN films deposited directly on Si substrates at reduced temperatures. The deposition technique used was HiPIMS, and the results indicated significant improvements in the film texture when comparing to the conventional Pulsed DC deposition process.

Keywords: Aluminum nitride, reactive sputtering, c-axis oriented films, tilted films, electroacoustic devices, piezoelectric materials, Aluminum Scandium Nitride, HiPIMS, high-k dielectric

Milena De Albuquerque Moreira, , Department of Engineering Sciences, Solid State Electronics, Box 534, Uppsala University, SE-75121 Uppsala, Sweden.

ISSN 1651-6214
ISBN 978-91-554-8995-3
urn:nbn:se:uu:diva-229588 (http://urn.kb.se/resolve?urn=urn:nbn:se:uu:diva-229588)

“What we know is a drop,
what we don’t know is an ocean.”

(Isaac Newton)

List of Included Papers

This thesis is based on the following papers, which are referred to in the text by their Roman numerals.

I **M. A. Moreira**, T. Törndahl, I. Katardjiev, T. Kubart, “Thin AlN films deposited by reactive HiPIMS and Pulsed DC sputtering: a comparative study,” (Manuscript to be submmited).

II **M. Moreira**, J. Bjurström, I. Katardjiev, and V. Yantchev, "Efficient RF voltage transformer with bandpass filter characteristics," *Electronics Letters,* vol. 49, pp. 198-199, 2013.

III J. F. Souza, **M. A. Moreira**, I. Doi, J. A. Diniz, P. J. Tatsch, and J. L. Gonçalves, "Preparation and characterization of high-k aluminium nitride (AlN) thin film for sensor and integrated circuits applications," *Physica Status Solidi (c),* vol. 9, pp. 1454-1457, 2012.

IV **M. Moreira**, J. Bjurström, I. Katardjiev, and V. Yantchev, "Aluminum scandium nitride thin-film bulk acoustic resonators for wide band applications," *Vacuum,* vol. 86, pp. 23-26, 2011.

V **M. Moreira**, J. Bjurström, T. Kubart, B. Kuzavas, and I. Katardjiev, "Synthesis of c-tilted AlN films with a good tilt and thickness uniformity," in *IEEE International Ultrasonics Symposium Proceedings*, 2011, pp. 1238-1241.

VI **M. A. Moreira**, I. Doi, J. F. Souza, and J. A. Diniz, "Electrical characterization and morphological properties of AlN films prepared by dc reactive magnetron sputtering," *Microelectronic Engineering,* vol. 88, pp. 802-806, 2011.

Author’s contribution

I	Part of planning and analysis. Major part of thin films deposition (Pulsed DC and HiPIMS) and measurements. Significant part of writing.
II	Minor part of planning. Involved in fabrication and measurements. Minor writing.
III	Minor part of planning. Major part of synthesis and characterization of AlN for the application as the transistor gate. Minor writing.
IV	Part of planning. Involved in synthesis and characterization of AlScN films. Involved in fabrication and characterization of FBARs. Minor writing.
V	Minor part of planning. Involved in thin films depositions and measurements. Minor writing.
VI	Part of planning. All fabrication and measurements. Significant part of writing.

Conference Contributions

i. Tomas Kubart, Ilia Katardjiev, **Milena Moreira**, "Thin AlN films deposited by reactive HiPIMS and pulsed DC sputtering - a comparative study," presented at *14th International Conference on Plasma Surface Engineering (PSE 2014)*, Garmisch-Partenkirchen, Germany, 2014.

ii. J. Olivares, M. M. Ramos, E. Iborra, M. Clement, T. Mirea, **M. Moreira**, I. Katardjiev, "IR-reflectance assessment of the tilt angle of AlN-wurtzite films for shear mode resonators," presented at *European Frequency and Time Forum & International Frequency Control Symposium (EFTF/IFC)*, Prague-Czech Republic, 2013.

iii. **M. A. Moreira**, J. Bjurström, V. Yantchev, I. Katardjiev, "Microacoustic voltage transformer with bandpass filter characteristics," presented at *IEEE International Ultrasonics Symposium (UFFC-IUS)*, Prague-Czech Republic, 2013.

iv. **M. A. Moreira**, J. Bjurström, V. Yantchev, I. Katardjiev, "Synthesis and characterization of highly c-textured $Al_{(1-x)}Sc_xN$ thin films in view of telecom applications," presented at *European Material Research Society E-MRS*, Strasbourg-France, 2012.

v. **M. A. Moreira**, J. Bjurström, V. Yantchev, I. Katardjiev, "Synthesis of wurtzite $Al_{(1-x)}Sc_xN$ thin films," presented at *IEEE International Ultrasonics Symposium (UFFC-IUS)*, Dresden-Germany, 2012.

vi. J. F. Souza, **M. A. Moreira**, I. Doi, J. A. Diniz, P. J. Tatsch, "Preparation and characterization of high-k Aluminum nitride (AlN) thin film for sensors and integrated circuits applications," presented at *International Conference on the Formation of Semiconductor Interfaces (ICFSI-13)*, Prague-Czech Republic, 2011.

vii. **M. Moreira**, J. Bjurström, T. Kubart, B. Kuzavas, I. Katardjiev, "Synsthesis of highly textured w-AlN thin films with a tilted c-axis having good tilt and thickness uniformity," presented at *IEEE International Ultrasonics Symposium (UFFC-IUS)*, Orlando-USA, 2011.

viii. **M. A. Moreira**, I. Doi, J. F. Souza, J. A. Diniz, "Electrical characterization and morphological properties of AlN films prepared by dc reactive magnetron sputtering," presented at *Materials for Advanced Metallization (MAM)*, Mechelen-Belgium, 2010.

ix. **M. A. Moreira**, I. Doi, J. F. Souza, J. A. Diniz, "Electrical properties of AlN MIS capacitors prepared by DC reactive magnetron sputtering technique," presented at International Conference on Electronic Materials (IUMRS-ICEM), Seoul-Korea, 2010.

Contents

List of figures

List of tables

Symbols and Abbreviations

A	Capacitor area
AC	Alternating current
ADS	Advanced Design System
$Al_{(1-x)}Sc_xN$	Aluminum Scandium Nitride
Al_2O_3	Aluminum oxide (or alumina or sapphire)
AlN	Aluminum nitride
Ar	Argon
B	Boron
BAW	Bulk acoustic wave
C	Capacitance
C_{33}	Stiffness
C_{fb}	Flat-band capacitance
C_{max}	Maximum capacitance
C_{min}	Minimum capacitance
Cr	Chromium
C-V	Current-voltage
CVD	Chemical vapour deposition
d	Diameter of the gas particles
DC	Direct current
e_{33}	Piezoelectric constant
ECR	Electron cyclotron resonance
EISFET	Electrolyte insulator semiconductor field effect transistor
EOT	Equivalent oxide thickness
ERDA	Elastic recoil detection analysis

FBAR	Film bulk acoustic resonator
FOM	Figure of merit
f_p	Parallel resonance frequency
f_s	Series resonance frequency
FWHM	Full width at half maximum
G_m	Transconductance
HCM	Hollow cathode magnetron
HfO_2	Hafnium dioxide
HiPIMS	High power impulse magnetron sputtering
IC	Integrated circuit
ICP	Inductively coupled plasma
I_{DS}	Drain-source current
IDT	Interdigital transducer
I_{off}	Current-off
IPVD	Ionized physical vapor deposition
ISFET	Ion sensitive field effect transistor
k	Dielectric constant
k_B	Boltzmann constant
k_{eff}^2	Effective electromechanical coupling
k_t^2	Electromechanical coupling coefficient or Intrinsic electromechanical coupling
MBE	Molecular beam epitaxy
MBVD	Modified Butterworth-Van Dyke
MEMS	Microelectromechanical systems
MFP	Mean free path
MIM	Metal-insulator-metal
MIS	Metal-insulator-semiconductor
MISFET	Metal insulator semiconductor field effect transistor
Mo	Molybdenum
N	Nitrogen

N_A	Substrate acceptor concentration
NB	Nowotny-Benes model
N_t	Charge trap density
p	Pressure
PBVT	Piezoelectric bandpass voltage transformer
PVD	Physical vapor deposition
PZT	Lead zirconate titanate
Q_B	Unloaded quality factor
Q-factor (or only Q)	Quality factor
Q_p	Quality factor at parallel resonance frequency
R_0	Shunt resistance
RF	Radio frequency
RFID	Radio-frequency identification
R_s	Series parasitic resistance
RTS	Radio triggered switch
Sc	Scandium
ScN	Scandium nitride
SiO_2	Silicon dioxide
S_t	Subthreshold swing
t	Thickness of the capacitor insulator
T	Temperature
Ta	Tantalum
tan δ	Dielectric losses
TCF	Temperature coefficient of frequency
Ti	Titanium
TiO_2	Titanium dioxide
V_{fb}	Flat-band voltage
V_{GS}	Gate-source voltage
VLSI	Very large scale integration
V_{th}	Threshold voltage

WLA	Wireless local area network
XRD	X-ray diffraction
Y	Yttrium
ZnO	Zinc oxide
ZrO_2	Zirconium dioxide
ε_0	Absolute dielectric permittivity
ε_{33}	Dielectric constant
ε_r	Relative dielectric permittivity
ϕ_{ms}	Work function metal-semiconductor

Chapter 1. Introduction

The requirements of the consumer market of high frequency devices, such as resonators and filters, have been more and more demanding over the last decades. Thus, a continuing enhancement of the devices' performance is required in order to meet these demands. In a macro view, changes in the design of the device can result in an improvement of its performance. In a micro view, the physical properties of the device materials also have a strong influence on its final performance. In the case of high frequency devices based on piezoelectric materials, a natural way to improve their performance is through the improvement of the properties of the piezoelectric layer.

This thesis summary presents the results from experimental studies on the synthesis of Aluminum Nitride (AlN) thin films in view of telecom, microelectronic and sensor applications. Thus, the main objective of this thesis is to custom design the functional properties of AlN to best suit these for the specific application in mind. This is achieved through careful control of the crystallographic structure and texture as well as film composition. Foremost, why is AlN the material of choice for this work?

AlN is a well-known and established compound among other piezoelectric materials. It is an III-V compound semiconductor with hexagonal wurtzite structure and unique electronic properties such as [1-5]:

- Wide bandgap (6.2 eV),
- High thermal conductivity (2 $W.(cm.K)^{-1}$, comparable to pure Al),
- High electrical resistivity (1 x 10^{16} Ω.cm), and
- High resistance to breakdown voltage (5 x 10^5 V/cm).

Moreover, AlN is also an interesting material due to its piezoelectric and electroacoustic properties, for instance [2-4, 6, 7]:

- High quality factor (around 3000 at 2 GHz for bulk acoustic wave devices (BAW)),
- Moderate coupling coefficient (6.5% for BAW),
- Moderate piezoelectric constant (e_{33}, 1.55 C/m^2),
- High acoustic velocity (11300 m/s for BAW), and
- Low propagation losses.

Besides its intrinsic characteristics, AlN thin films are chemically stable and compatible with the IC-fabrication technology. The combination of all

these properties makes AlN one of the most used piezoelectric materials for the fabrication of electroacoustic devices, eg thin film BAW bandpass filters.

Molecular beam epitaxy (MBE) [8, 9], chemical vapour deposition (CVD) [10-12] and sputtering [1-4, 13-15] are some of the techniques commonly used to grow AlN films. The choice of the deposition technique is defined by the specific application. Noteworthy, MBE and CVD require high deposition temperatures, making them incompatible with the fabrication of electroacoustic devices. In this sense, sputter-deposition of AlN films is a suitable choice for the fabrication of these devices since it requires relatively low deposition temperatures.

Some advantages of the reactive sputtering technique compared to other deposition techniques are high deposition rates, excellent texture control and film uniformity. AlN thin films can be deposited by means of several variants of the sputtering technique such as:

- High power impulse magnetron (HiPIMS) [16, 17],
- Direct current (DC) magnetron [1, 3, 16],
- Pulsed DC magnetron [4, 17], and
- Radio frequency (RF) magnetron [14, 18].

The sputtering methods used in this work are DC, Pulsed DC and HiPIMS[1].

The properties of the piezoelectric layer define the performance of the electroacoustic device, since these properties impact directly on the electroacoustic properties (insertion loss, coupling coefficient, quality factor, bandwidth, dielectric constant, etc.). Therefore, a careful control of the process deposition conditions is a requirement for the growth of highly textured (c-axis oriented) AlN films (*Figure 1*).

One way to evaluate the texture of c-axis oriented AlN film is by the analysis of the rocking curve of its (002) X-ray diffraction (XRD) peak. The better the orientation of the film, the smaller the full width at half maximum (FWHM) of the (002) peak, thus indicating better alignment of the c-axis of the individual grains with the surface normal.

The electromechanical coupling, which is a measure of the conversion efficiency between electric and mechanical energy, is highest for longitudinal deformation along the c-axis of wurtzite AlN. Noting that modern telecom applications require large bandwidths and that the bandwidth is proportional to the electromechanical coupling, it transpires that films with excellent c-texture are needed for such applications. Consequently, most commercial telecom devices make use of longitudinal bulk waves propagating along the c-axis. Electrical excitation is effected by an electric field also parallel to the c-axis (along the film thickness) for which reason such devices are said to make use of thickness excited

[1] Also known as HPPMS (high power pulsed magnetron sputtering).

longitudinal bulk waves. The term longitudinal denotes the direction of the particle displacement which is parallel to the wave vector as illustrated in *Figure 2*.

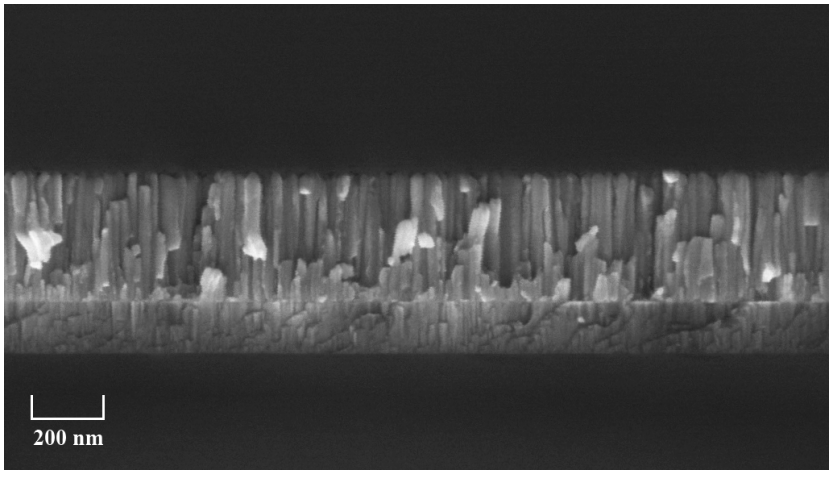

Figure 1. C-axis oriented AlN film deposited by Pulsed DC on top of a Mo layer.

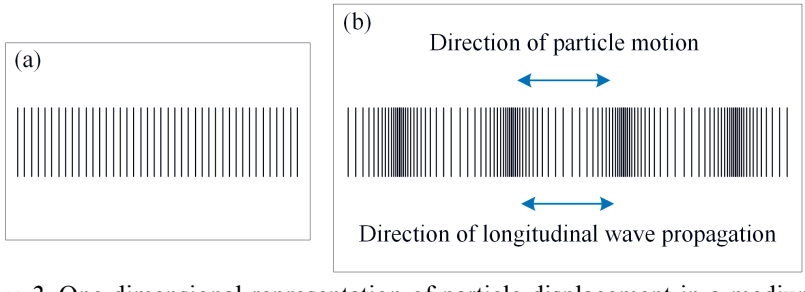

Figure 2. One dimensional representation of particle displacement in a medium (a) without any wave motion, and (b) with longitudinal wave propagation.

As indicated above, the primary use of the electroacoustic technology is its application in the telecom field (oscillators, filters, delay lines, and so on). However, there has been a growing use of thin film electroacoustic devices in sensing applications. This is due to their higher sensitivity, resolution as well as reliability when comparing with other type of sensors [19]. In the past few years thin film electroacoustic based sensors have been reported, for instance, pressure sensors [19, 20], gravimetric sensors [20], temperature sensors [19], gas flow sensors [21, 22] and biosensors [22-25].

Notwithstanding, the use of the thin film electroacoustic technology for sensors is not straightforward, particularly for sensors operating in liquid/viscous media, e.g. chemical and biochemical sensors. This is due to the fact that longitudinal and surface waves exhibit a considerable acoustic leakage into liquid/viscous media, ergo resulting in a loss of sensor

resolution. To this end, shear wave resonators are employed since shear waves do not propagate in liquids and hence exhibit considerably lower acoustic losses in such media. Unfortunately, the piezoelectric constants of AlN are such that electrical excitation of shear waves is only effected by an electric field having a non-zero angle with the c-axis. More specifically, when this angle is $\theta = 90^{o}$ (i.e. a-textured films) the mode is pure shear (*Figure 3*). In the case where θ is smaller than 90^{o} the mode excited is quasi-shear, that is, it has one shear and one longitudinal components. The latter declines rapidly with θ and hence at angles larger, say, than 20^{o} the longitudinal excitation is negligible and hence the acoustic leakage associated with the longitudinal component is also negligible. Ideally, one would like to use the pure shear mode, but the technological difficulties associated with growing unipolar a-textured films render this approach impractical. For this reason, focus has shifted towards the synthesis of textured AlN films with a tilted c-axis (*Figure 4*) which in turn allows thickness excitation of quasi-shear waves. This thesis studies both the nucleation and growth mechanisms that allow the synthesis of thin AlN films with a tilted c-axis in view of shear wave electroacoustic sensors.

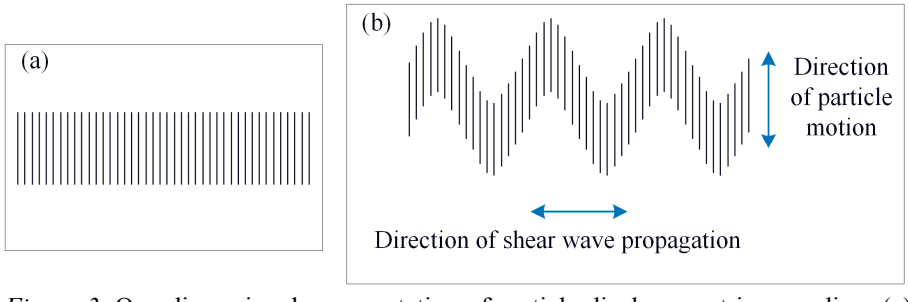

Figure 3. One dimensional representation of particle displacement in a medium (a) without any wave motion, and (b) with shear thickness wave propagation.

The above two examples illustrate how desired functional (electroacoustic and dielectric) properties are achieved through control of both the crystallographic structure and texture of the films. Another area of study in this thesis is enhancing the functional properties of AlN through compositional changes. To this end, recent studies demonstrate improvement of various electroacoustic and piezoelectric properties of AlN films by doping these films with metalloids, such as B [26-28], and transition metals, like Ti [29], Sc [30, 31], Y [32], Cr [33, 34] and Ta [35]. Thus, in this thesis we demonstrate for the first time the potential of highly c-textured thin AlScN films for wideband telecom applications. This, along with other works in the thesis, represent a third area of studies where the enhanced functional properties of the films thus synthesized are demonstrated experimentally through the fabrication of specific devices and components,

which are subsequently characterized electrically, and thus complete the cycle of the research.

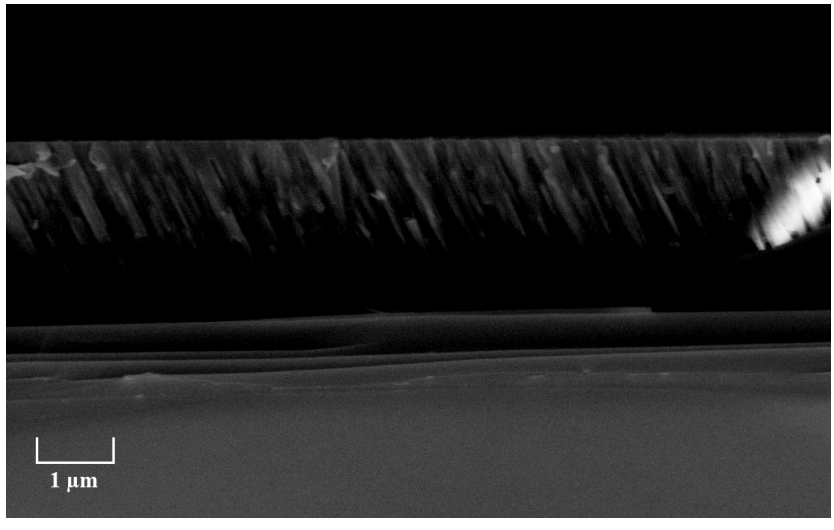

Figure 4. C-axis tilted AlN film deposited by Pulsed DC on Si substrate.

In the following chapters, a brief background about the underlying concepts will be presented followed by a description of the experimental procedures adopted. Subsequently, the main results of the research will be presented and discussed, along with a summary of the included papers. Finally, the conclusions from the work here are presented.

Chapter 2. Theoretical background

As previously mentioned, the goal of this work is the improvement of AlN properties in view of sensors and telecom applications. To this end, many different aspects of synthesis and characterization of AlN films were studied. For instance:

- Enhancement of the piezoelectric properties of c-axis oriented AlN films by doping,
- Alternative approach to deposition of c-axis tilted AlN films,
- High-k AlN films,
- Fabrication of electroacoustic devices, and
- Improvement in the nucleation layer by the use of ion assisted sputter deposition (HiPIMS).

Since this work includes various aspects related to AlN thin films, the purpose of this chapter is to bring up the discussion by presenting a brief overview of the different topics discussed in this summary. Furthermore, a literature review and the state-of-art of related research are presented to some extent.

2.1. C-axis oriented AlN

The electromechanical coupling coefficient k_t^2 is a numerical value that represents the efficiency of piezoelectric materials to convert electrical into acoustic energy (and vice versa) for a given acoustic mode. Therefore, the higher the k_t^2, the higher the electrical-acoustic energy conversion. The piezoelectric response of wurtzite AlN is the integral effect of the individual dipole contributions of all the grains comprising the film. Thus, a highly c-axis oriented film yields a high k_t coefficient since the grains will be aligned along the same direction, collaborating then to the same sign to the piezoelectric response (*Figure 5*) [36].

Sputtered AlN films can grow in a crystalline or an amorphous phases, and furthermore the crystalline films can grow in textured and non-textured ways [3]. One further peculiarity of wurtzite AlN is that it is a polar material. In this context it is equally important that c-textured films are in addition unidirectional in order to be piezoelectric. The Al atoms sputtered from the

Al target will react with the N atoms and ions present in the plasma, creating AlN clusters[2]. Thus, a good control of the deposition parameters is crucial in order to obtain highly c-axis textured films.

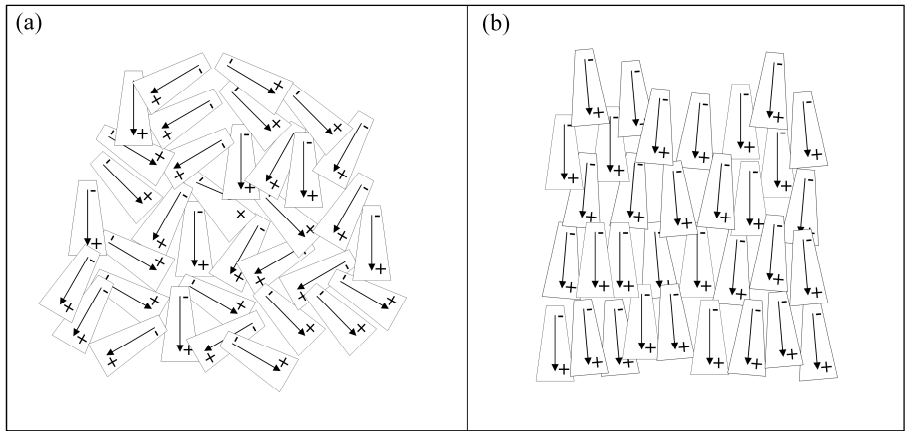

Figure 5. Schematic of the dipoles distribution along a piezoelectric net: (a) grains aligned in various directions, and (b) grains aligned along the same direction.

In the case of sputtered films, some of the most important deposition parameters to consider are: substrate temperature, processing pressure, Ar/N_2 flow rate, discharge power and target-to-substrate distance. It is essential to provide the adatoms[3] with the right amount of energy [6, 36]. To this end, the optimal balance between these deposition parameters must be achieved[4]. Obviously, this balance varies for different experimental setups.

The mean free path[5] (MFP) of a sputtered atom is given by

$$MFP = \frac{k_B T}{\sqrt{2}\pi d^2 p} \qquad (1)$$

where k_B is the Boltzmann constant (~1.38×10^{-23} J/K), T is the temperature (in Kelvin), d is the diameter of the gas particles (in meters) and p is the pressure (in Pascals). As indicated by the above equation, the MFP is influenced by both pressure and temperature. To further illustrate the influence of pressure, the MFP of the sputtered Al atoms at a pressure of 20 mTorr is around 1 cm (at room temperature); on the other hand, the MFP is equivalent to 10 cm at a pressure of 2 mTorr [37].

[2] A cluster has an intermediate size between a single crystal and a bulk solid material.
[3] Adatom is a non-absorbed atom lying on the crystal surface and that can migrate over it.
[4] Other important parameters to consider are film thickness, substrate bias and deposition rate [6].
[5] Mean free path is the average distance that an atom can move without colliding at another atom.

At low gas pressures, the number of collisions and scattering by the gas molecules is also low (larger MFP), which means that the atoms sputtered from the target will retain a significant fraction of their initial kinetic energy when arriving at the substrate surface. This in turn favors the growth of wurtzite structure of AlN [3] since this relatively high kinetic energy enhances the adatom mobility, ergo making them diffuse over the surface [38] and eventually finding a low energy lattice site. Noteworthy, the adatom mobility can also be enhanced by increased substrate temperature.

The growth of c-axis textured films is dependent not only on the deposition conditions. The substrate material and its crystallographic structure also play an important role in the film growth. Thus, AlN films deposited on top of highly textured metal films having a hexagonal surface symmetry show higher c-axis texture due to crystallographic similarity [39]. Besides, the roughness of the bottom material should be considered since it can influence the adatom mobility of sputtered AlN. Comparing films prepared under the same deposition conditions but on materials with different roughness/smoothness, the adatom mobility is much higher on smooth surfaces. Thus, in order to provide the same adatom mobility on rough surfaces, it is necessary to improve the kinetic energy of the sputtered particles (by means of increasing the deposition temperature, for example). Another important aspect of surface roughness is that nucleation of AlN grains with the c-plane parallel to the surface is thermodynamically the most energetically favorable. Hence, the FWHM of the rocking curve is proportional to the surface roughness, or in other words high roughness results in a poor c-texture. This fact can also be used for the growth of AlN films with a tilted c-axis as discussed next.

2.2. Tilted AlN

For some specific applications, such as biosensors based on the electroacoustic technology and operating in liquid/viscous media, AlN films with a tilted c-axis are more suitable than the c-axis oriented ones [22-25, 40]. Resonators using the shear wave mode are most suited for such applications due to the decrease of acoustic losses when comparing with the longitudinal wave mode ones. The reason for this is that shear waves do not propagate in liquids and hence acoustic leakage typical for longitudinal waves is totally eliminated when employing shear waves. Unfortunately, shear waves cannot be excited in c-textured AlN films with an electric field along the film thickness while lateral field excitation exhibits extremely low couplings. Therefore, for thickness excitation of shear waves, films with a tilted c-axis are required.

There are a variety of methods available to deposit tilted AlN films. Some of them are (see *Figure 6*):

i. Off-axis (or off-normal) deposition [41, 42],
ii. Tilted substrate deposition [43, 44],
iii. Tilted and off-centered target deposition [45, 46], and
iv. Two-stage deposition process [40].

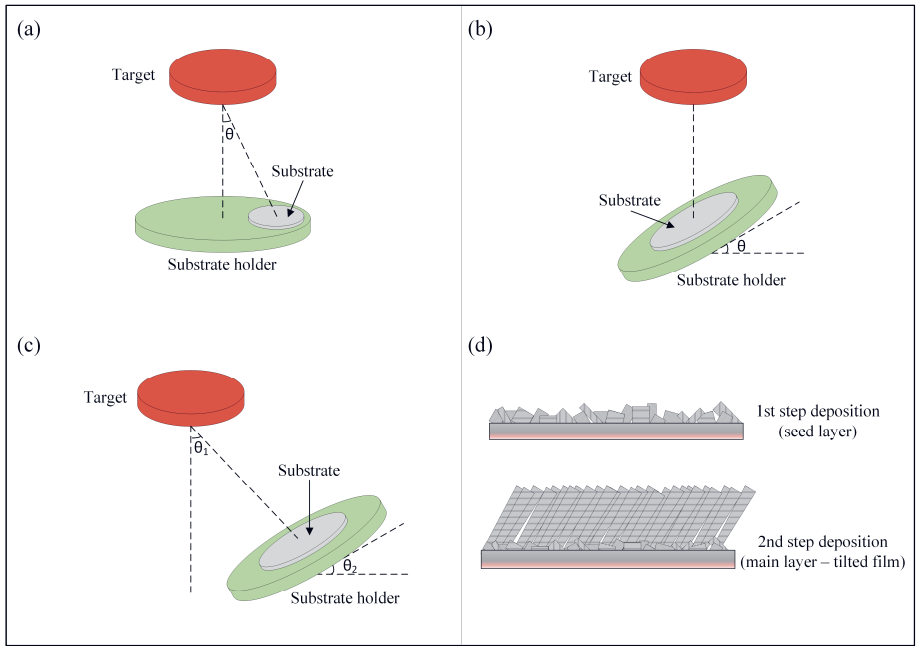

Figure 6. Simplified schematic of different deposition setups for tilted films: (a) off-axis deposition, (b) tilted substrate, (c) tilted and off-centered, and (d) two-stage deposition process.

The three first methods require modifications in the standard setup of sputtering systems, whereas the latter one does not require any additional hardware changes. The general concept of these methods will be briefly discussed in here.

As in any sputter-deposition process, the deposition conditions strongly influence the growth of tilted films. It is well established that the adatom mobility plays an important role in obtaining highly textured films during sputter deposition [42, 44, 46-48]. Hence, in order to create conditions favorable for the nucleation of non c-oriented grains, adatom mobility needs to be suppressed. This is the reason the Uppsala deposition process consists of the following two steps, as presented in Paper V. An initial thin and "non-textured" seed layer is grown (*Figure 7*) by operating at relatively high process pressure and keeping the substrate at room temperature. All this

results in a complete thermalization of the sputtered atoms, and hence in operating the deposition process in the diffusion limited regime. The resulting seed layer exhibits different textures, most notably (103) and (002). Once the seed layer has been deposited, growth of the film proceeds at low process pressures and elevated substrate temperature, both of which favor good crystal growth. The succeeding film growth however has no chance to proceed differently but to follow the crystallographic texture of the seed layer. In addition, the low pressure deposition in combination with a small target-to-substrate distance also yield a directional deposition flux. This results in competitive column growth, i.e., cones having the c-axis along the direction of the deposition flux grow fastest. In turn, this results in a film with c-tilt lying in the plane of the deposition flux at any given point on the substrate.

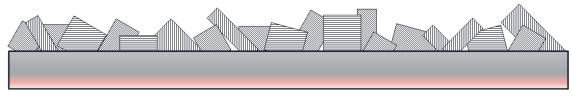

Figure 7. Schematic of the nucleation layer with random crystal planes.

In the three first methods mentioned previously (i-iii), the tilted columns have a preferential growth due to the alignment with the tilted flux. This is very similar to what occurs during glancing angle deposition of sculptured thin films [49]. In the method (iv), the seed layer has a (103) dominant population rather than a totally random film [40]. Even though there is no intentional tilt of the flux, the magnetron disposition at the target generates a race track, which in turn provides the tilted flux direction towards the substrate (see *Figure 6d*).

2.3. Doped AlN

The constantly increasing requirements for stringent specifications of the telecom market requires continuous improvement in the performance of high frequency devices. To this end, basically two steps can be considered: (i) improvements in device design, and (ii) enhancement of the properties of the constituent materials. Both steps aim at advances in the devices performance by achieving lower losses, higher resolution, higher bandwidth, lower production costs, lower capacitance parasitic, and so on.

One of the goals of this work is to improve the piezoelectric properties of AlN films. It is well-known that AlN possesses various properties suitable for high frequency devices (chemical stability, compatibility with IC-technology process, high quality factor, etc.). Owing to this, AlN is a promising material for use in high frequency devices (resonators, filters and oscillators, for instance). Although, the relatively low piezoelectric response

does restrict its use in some applications, such as filters that require larger bandwidths.

It has been recently reported that a doping of AlN films with certain chemical elements can be beneficial to the improvement of its piezoelectric properties [26-35, 50-52]. However, this process is not straightforward. It is necessary to synthesize the new material (doped AlN) in order to find the optimized doping concentration and deposition conditions (and evidently this optimization varies for different dopant materials). This means that, even if the best deposition conditions are well-known for a certain equipment to achieve highly textured AlN films, the same conditions cannot be directly applied for the new material (AlXN[6]). For instance, gas flows, deposition temperature and target(s) power(s) must be optimized.

Nowadays there are four main methods to sputter AlXN thin films (*Figure 8*):

i. Concentric ring-shaped targets [29],
ii. Dopant inserts in the Al target [33, 34],
iii. Alloyed Al target [51], and
iv. Co-sputter by use of two different targets [52].

The disadvantage of the three first methods (i-iii) is that the constituents ratio Al/X is fixed at all depositions. This disadvantage does not exist for the method (iv), where the ratio Al/X can be modified by changing the sputter power of each target (Al and X material).

Specifically for electroacoustic devices based on AlN thin films, a dopant that has attracted a lot of attention nowadays is Sc. Ab-initio calculations and experimental results suggest the enhancement of the piezoelectric properties of AlN by doping it with a certain amount of Sc [7, 53]. This work experimentally investigated the synthesis of highly c-textured aluminum scandium nitride[7] ($Al_xSc_{(1-x)}N$) thin films as well as evaluated their piezoelectric properties (Paper IV). The deposition method chosen is co-sputtering (*Figure 8d*).

Scandium nitride (ScN) is a III-V nitride with rock-salt structure (non-polar[8]), and AlN is III-V nitride with wurtzite structure (polar[9]). There is a transition region between wurtzite and rock-salt structures by doping AlN films with Sc. Some authors support that this intermediate phase state is responsible for the improvement in the piezoelectric response of the film [30].

[6] AlXN is written in here as a simplified way to refer to doped AlN films. "X" can be any dopant.
[7] It is usual to find in the literature the nomenclature scandium aluminum nitride ($Sc_{(1-x)}Al_xN$) for the same material.
[8] In a non-polar structure there is an equal distribution of charges in the molecule.
[9] In a polar structure there is a non-similar distribution of charges, i.e., there is a positive charge in one end of the molecule and a negative charge in the other end.

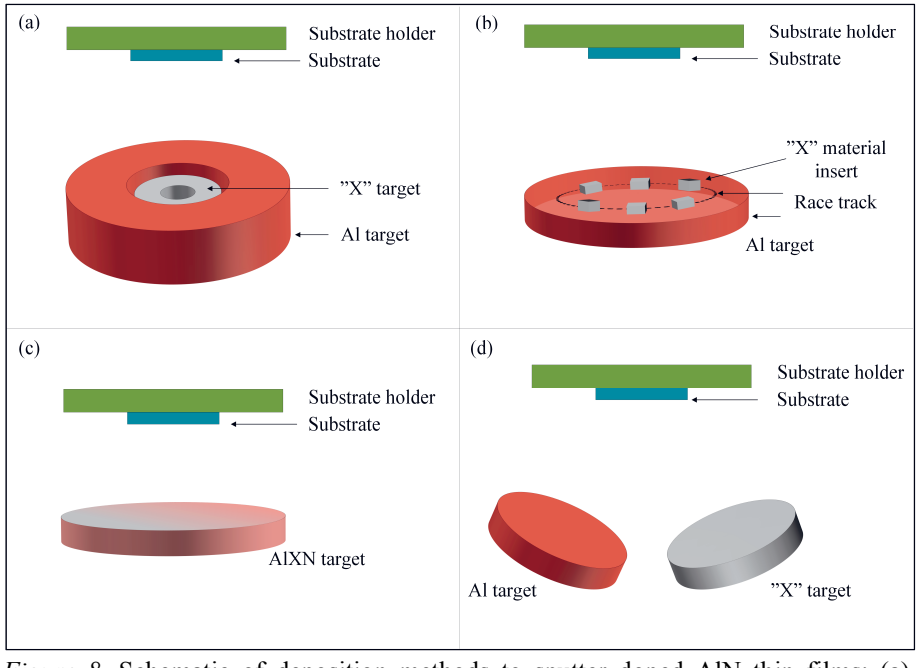

Figure 8. Schematic of deposition methods to sputter doped AlN thin films: (a) concentric ring-shaped targets, (b) dopant inserts into the Al target, (c) alloyed Al target, and (d) co-sputter with two different targets.

The electromechanical coupling (k_t^2) is directly related to the properties of the piezoelectric films. The equation that defines k_t^2 can be written as

$$k_t^2 = \frac{{e_{33}}^2}{\left(C_{33}+\frac{{e_{33}}^2}{\varepsilon_{33}}\right)\varepsilon_{33}} \qquad (2)$$

where e_{33}, C_{33} and ε_{33} are the piezoelectric constant, stiffness and dielectric constant, respectively. It can be seen from the previous equation that an increase in the piezoelectric constant and a decrease in the stiffness of the material contribute to the improvement of k_t^2. Both goals can be achieved by doping AlN films with Sc, which has been proved theoretically [7, 53] and experimentally [30, 31, 51, 52].

Noteworthy, an increase of 500% in the piezoelectric response of AlN films doped with Sc was experimentally demonstrated [30]. Unfortunately, other properties such as the acoustic losses and sound velocity somewhat deteriorate (which can be expected by the decrease of the stiffness coefficient). With respect to filter design an important figure of merit is the product k_t^2 x Q. Thus, in this case a tradeoff between k_t^2 and Q is sought so that the product between these is higher than that of pure AlN.

2.4. Electroacoustic devices

Electroacoustic devices can be designed in various ways in order to explore different propagation modes. Some of these modes are [54]:

- Longitudinal BAW,
- Shear BAW,
- Surface acoustic wave,
- Shear-horizontal acoustic plate mode,
- Surface transverse wave,
- Love wave, and
- Flexural plate wave.

The structures of different types of electroacoustic devices differ in terms of the active layer material (piezoelectric materials) and the particle displacement relative to the wave propagation direction.

A range of these acoustic modes are already exploited in the telecom market, where they have been used as filters and oscillators, for instance. However, as mentioned before (Chapter 1), there has been a growing interest in their application in the sensing field. In this case, the piezoelectricity is used in an indirect[10] way [50]: sensing is achieved through perturbation of the acoustic wave that propagates through the piezoelectric layer. This perturbation may be the result of a biochemical reaction or a temperature change, or strain due to external force, etc. Typically, this perturbation results in a frequency shift and/or change in the propagation losses, which subsequently are calibrated by the readout electronics to provide the sensing information (temperature, pressure, viscosity, mass, etc). Noteworthy, the overall performance of the resonator of the electroacoustic sensor will affect the design of the final readout circuit insofar as quality factor[11] and electromechanical coupling define sensitivity and resolution of the sensor [50].

The design of the electroacoustic sensors is driven by their final application. For instance, the choice of the acoustic propagation mode and the active layer material will determine whether the sensor can be used in gaseous or in-liquid media. As an example, one can mention the use of tilted AlN films (instead of c-axis oriented) in the shear wave mode (instead of the longitudinal one) is the most suitable for in-liquid media applications [23, 40-42, 44].

[10] In the direct use, the piezoelectric concept is straightforward: the sensing parameters causes a mechanical deformation in the piezoelectric layer, and consequently an electrical signal will be generated.

[11] The quality factor of an oscillating system is defined as the ratio between the energy stored and the energy dissipated by the system during the one oscillation cycle [54].

In this work, electroacoustic devices were used as a tool to study the effects in the electroacoustic properties of AlN films by doping these films with different Sc concentrations (Paper IV). FBAR (film bulk acoustic resonator) was the electroacoustic device fabricated.

2.5. High-k AlN

It is well known that the dimensions of the devices based on the transistor technology are continuously scaling down. For this reason, the thickness of the gate dielectric must follow the re-scaling of the transistors in order to keep the same capacitance between gate and the channel regions. To illustrate the relationship between gate thickness and capacitance, the gate dielectric can be modeled in a simplified way as a parallel plate capacitor, to which the capacitance C is given by

$$C = \frac{k\,\varepsilon_0\,A}{t} \qquad (3)$$

where k is the dielectric constant of the gate material, ε_0 the absolute dielectric permittivity, A is the capacitor area and t is the thickness of the capacitor insulator (in this case, the gate layer).

The most used gate dielectric in the Si based VLSI (very large scale integration) technology is SiO_2, which already reached its physical thickness limit in the scaling down process. For gate thickness scales below 2 nm the leakage current[12] is strongly pronounced due to the tunneling current effect, driving the device to a worsened performance because of the increased power consumption and lowered reliability[13]. An alternative is to increase the dielectric constant coefficient k, thus having a degree of freedom to work with thicker gate layers while keeping a high capacitance. To this end, materials with higher dielectric constants to replace the SiO_2 gate have drawn attention in the last few years. Some of these materials are Al_2O_3, HfO_2, ZrO_2, TiO_2 and AlN [55, 56].

However, there are some technological problems to handle when using oxides as gate dielectric material, such as the appearance of SiO_2 or silicates in the interface layer between the gate oxide and Si substrate. These interfacial layers have a lower-k coefficient, leading to a decrease in the overall capacitance density [55]. In this sense, nitrides and oxi-nitrides have been calling more attention as an alternative to replace SiO_2 as the gate

[12] Also called as off-current, it is defined as the small amount of current that continues to flow between source and drain after the voltage is turned off.
[13] The reliability of a device describes its capacity in working for certain period of time under stated conditions.

dielectric layer. Thus, AlN films stand as a suitable material since the nitride film suppress the rise of interfacial layers between high-k dielectric and Si substrate (mostly due to the high amount of oxidized elements with oxide gate films). An experimental work to evaluate the possibility to use AlN as gate dielectric is presented in Paper III.

2.6. High power impulse magnetron sputtering (HiPIMS)

Magnetron sputtering have been used in a wide range of research and industrial applications over the last decades. However, the continuous and increasing demand for new materials and improved properties leads to the need for development of new deposition techniques in order to achieve better control of the deposition process. To this end, techniques to increase the degree of ionization of sputtered species have been studied and developed [57], and the HiPIMS is one of those. Considering that HiPIMS is an emerging technique and not fully explored yet, a short and brief description of this sputtering process will be presented in here.

The PVD (physical vapor deposition) methods characterized by a flux of ions higher than the flux of neutrals of the deposited species are called IPVD (Ionized physical vapor deposition) [58, 59]. There are different methods among the IPVD technique, such as [59, 60]:

- Cathodic arc deposition,
- HCM (hollow cathode magnetron), and
- HiPIMS.

Alternative ways to enhance the ionization fraction in conventional magnetron sputtering is to use a supplementary ICP (inductively coupled plasma) or ECR (electron cyclotron resonance).

The common characteristic of the aforementioned methods is the possibility of a good control of energy and direction of the sputtered material. Notwithstanding, comparing with other IPVD methods, an advantage of HiPIMS is its simplicity since any sputtering machine based on magnetrons can be turned into a HiPIMS system by only replacing the power supply.

The basic concept of HiPIMS is the delivery of a high degree of ionization to the system by means of a high density plasma. To this end, the power supply should deliver pulses in the order of $kW.cm^{-2}$ (the power supplies used in conventional magnetron sputtering systems provide pulses in the range of a few tens $W.cm^{-2}$) [59, 61]. Comparing the values of plasma densities for both techniques, conventional magnetron sputtering delivers

electron densities in the range $10^{14} – 10^{16}$ m^{-3}, while this values for HiPIMS are commonly in the range $10^{18} – 10^{20}$ m^{-3} [57, 59].

High density plasma is achieved by means of high power pulses delivered to the magnetron at low frequency and low duty cycle[14]. In other words, the HiPIMS pulse can be compared to an impulse: pulse with very high amplitude and long time gap between the pulses [61]. Noteworthy, due to the high electrical power delivered to the target surface, a low duty cycle is mandatory in order to avoid target overheating.

As in any sputtering technique, the properties of the films deposited by HIPIMS can be adjusted by tuning the deposition parameters. Pressure, temperature, substrate, target power, etc., influence the characteristics of the films. However, it is important to highlight here the enhancement that the increased ionization gives to the films properties. Improvements in roughness, density, adhesion and hardness are observed when comparing HiPIMS and conventional magnetron sputtering techniques [61].

One drawback of the HiPIMS technique is the reduction of the deposition rate (compared with Pulsed DC depositions under similar conditions[15], see *Figure 9*). Some authors explain this behavior by the phenomenon of back attraction of the sputtered and highly ionized species back to the target [16, 59, 61]. Alternative setup arrangements have been studied in order to increase the deposition rate [57].

There are just a few studies reported in the literature presenting AlN films deposited by HiPIMS. The work presented in Paper I intends to contribute in an overall analysis of AlN films sputtered by HiPIMS. Moreover, Paper I presents and discuss the results of highly c-axis textured AlN films deposited by this technique.

[14] Duty cycle is the fraction of time in which the signal (pulse) is active (on) within one period.

[15] Refer to Paper I for further information regarding the deposition parameters of both processes.

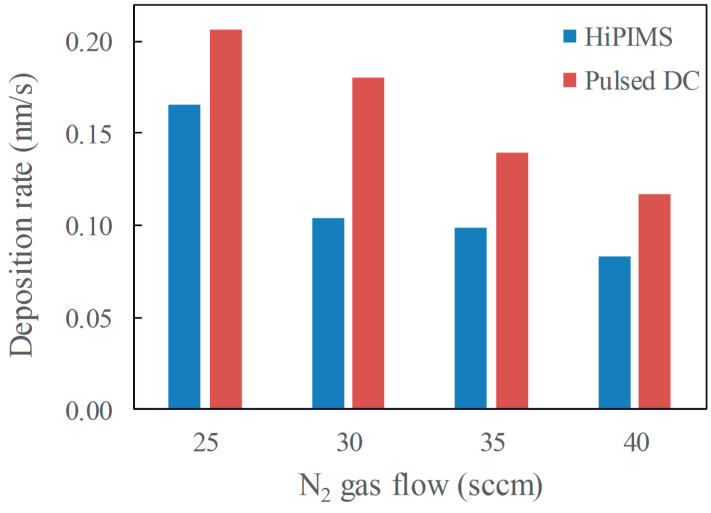

Figure 9. Comparative plot of the deposition rate of AlN films deposited under similar conditions by HiPIMS and Pulsed DC.

Chapter 3. Results and Discussions

This chapter highlights and discusses more deeply some of the main achievements of this work regarding the synthesis and characterization of thin piezoelectric films as this represents the main thrust of this thesis. It does not mean though that the topics that are not included in here are less significant. Notwithstanding the results and discussions in the papers, some of the results presented in this chapter have not been published yet. Therefore, the discussion based on these non-published results intends to complement the published work as well as, in an overall analysis, contribute to the field of piezoelectric materials for high frequency applications.

An extended summary of all results in this thesis are presented in Chapter 4.

3.1. Synthesis and characterization of AlScN films

As previously mentioned, the $Al_{(1-x)}Sc_xN$ films investigated in this work were deposited by the Pulsed DC co-sputtering method (refer to *Figure 8d*). The total amount of Sc in each film was controlled by the power delivered to the Sc target. The composition of the films was investigated by Elastic recoil detection analysis (ERDA) and the results of some $Al_{(1-x)}Sc_xN$ films are presented in *Figure 10*.

In order to reach highly c-textured films, one important step in the synthesis of $Al_{(1-x)}Sc_xN$ films was the investigation of the optimal substrate temperature during deposition. To this end, one specific composition of $Al_{(1-x)}Sc_xN$ film was chosen (x = 0.09) and films were grown at different temperatures, in the range from room temperature up to 800 ^oC. The film texture was judged by the films' rocking curve (XRD analysis), where the FWHM[16] of each film was measured afterwards.

As indicated in *Figure 11*, there is an improvement at the FWHM by increasing the temperature up to 400 ^oC, at which the film reaches the best FWHM (lowest value). For temperatures higher than 400 ^oC the FWHM starts to deteriorate. Some authors explain this phenomenon by assuming that there is a threshold energy for the adatoms which defines the different

[16] The FWHM is calculated from the rocking curve (X-ray diffraction). The lower is the FWHM (narrower curve), the better is the film texture.

growth mechanisms, ergo the film texture [62, 63]. Still according to these authors, the increment of the adatom mobility at the substrate surface contributes not only to the preferential orientation growth (002 plane), but also to the grain coarsening. Depending of the overall energy delivered to the adatoms (around the threshold energy, for instance), the AlN (002) plane growth can be promoted and other crystal orientations suppressed.

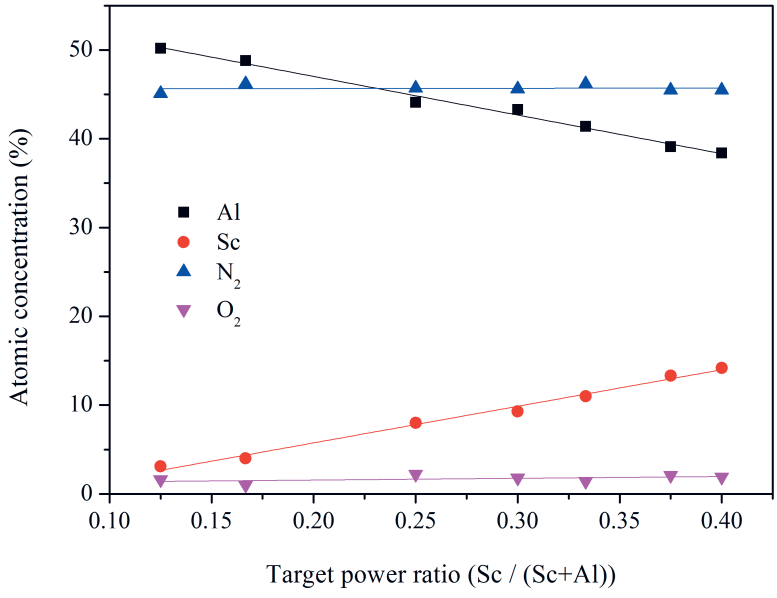

Figure 10. ERDA analysis of $Al_{(1-x)}Sc_xN$ films.

Therefore, the substrate temperature for the deposition of $Al_{(1-x)}Sc_xN$ films was set to 400 °C since the films deposited at this temperature presented the best results in terms of texture. Obviously this temperature is valid for a specific hardware setup (target-to-substrate distance, rotation speed of the target, substrate heating method, etc.) and deposition conditions (gas flow rate, target power, etc.). Most likely, for different hardware setups and deposition conditions there will be other optimal substrate temperatures for deposition of textured $Al_{(1-x)}Sc_xN$ films due to the differences in the overall balance of energy between the systems. A summary of the hardware setup and deposition conditions used in this work are listed in *Table 1*.

Noteworthy, substrate temperature studies were performed also for other $Al_{(1-x)}Sc_xN$ compositions. However, the temperature range variation was not as broad as for the $Al_{0.92}Sc_{0.09}N$ film. The temperatures used were 300 °C, 400 °C and 500 °C. Even though the film compositions were different, the results indicated 400 °C as the optimal substrate temperature for all cases.

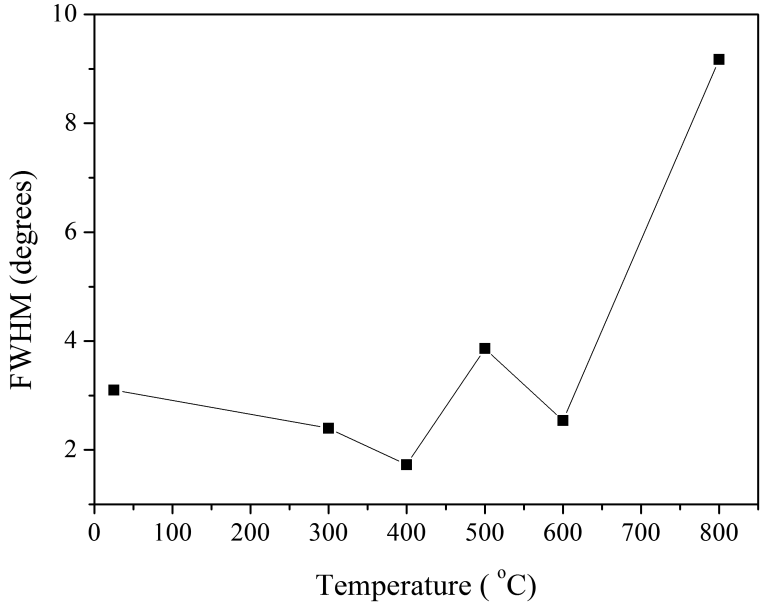

Figure 11. Influence of deposition temperature on the texture of AlScN (FWHM plot).

Table 1. Brief summary of the hardware setup and deposition conditions of $Al_{(1-x)}Sc_xN$ films.

Target-to-substrate distance	18 cm
Rotation speed	20 rpm
Substrate heating	Radiative heater
Base pressure	$< 2 \times 10^{-8}$ Torr
Deposition pressure	2.8 – 3.1 mTorr
Ar flow	30 sccm
N_2 flow	30 sccm

Another important step in the synthesis of $Al_{(1-x)}Sc_xN$ films was the investigation of the suitable substrate to grow the films. The initial tests were performed on Si and Si/Mo (300 nm) substrates.

On Si substrates, the films showed columnar structure but high FWHM (around 7°). This value is not acceptable for use in high performance devices, which require piezoelectric films with FWHM between 1° - 2°. A possible solution to this issue is the improvement in the nucleation layer of the $Al_{(1-x)}Sc_xN$ films deposited directly on Si. However, the target-to-substrate distance in the equipment used to deposit the films is high (see *Table 1*), which makes it more difficult to achieve higher adatom mobility over the substrate surface. In this work we suggest the use of HiPIMS

deposition to grow suitable nucleation layers for the $Al_{(1-x)}Sc_xN$ films (for further details see item 3.3 and Paper I.

Besides the films deposited directly on Si substrates, it was necessary to synthesize also the films deposited on top of a metal layer since the use of a bottom electrode is required for some devices applications. The metal used in here is Molybdenum (Mo) due to its intrinsic properties such as low acoustic attenuation and high electrical conductivity [64], which makes it a common choice as metal layer (electrode) for electroacoustic devices applications.

However, obtain highly textured films on top of Mo layer is not straightforward since there is a lattice mismatch between Mo and $Al_{(1-x)}Sc_xN$ structural planes. There are reports in the literature suggesting the use of a thin AlN seed layer underneath the Mo in order to improve the texture of the latter one [64, 65], ergo leading to an improvement in the texture of the main AlN layer. The same concept was used in this work in order to enhance the quality of $Al_{(1-x)}Sc_xN$ films deposited on top of Mo.

The beneficial effect of the AlN interlayer on the texture of $Al_{(1-x)}Sc_xN$ film is seen in *Table 2*, where the presented results refer to the composition x = 0.09 (deposition at room temperature). In *Figure 12* one can see a simplified schematic of the substrates and stacked layers used to grow $Al_{(1-x)}Sc_xN$ films. Noteworthy, in order to achieve the best quality $Al_{(1-x)}Sc_xN$ films, a study was carried out where the thicknesses of the AlN and Mo layers were systematically changed.

Table 2. FWHM (degrees) of $Al_{0.92}Sc_{0.08}N$ (002) and Mo (110) films.

	Mo (110)	**$Al_{0.92}Sc_{0.08}N$ (002)**
(a) Si / $Al_{0.91}Sc_{0.09}N$	-	6.7
(b) Si / Mo / $Al_{0.91}Sc_{0.09}N$	12	9.5
(c) Si / AlN interlayer / Mo / $Al_{0.91}Sc_{0.09}N$	3.2	3.1

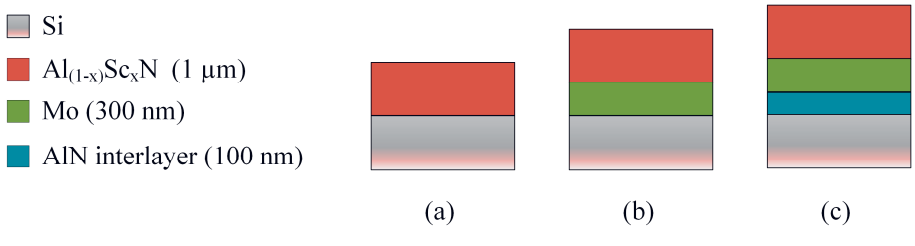

Figure 12. Simplified schematic the substrates and stacked layers used to grow $Al_{(1-x)}Sc_xN$ films: (a) Si, (b) Si/AlN interlayer and (c) Si/AlN interlayer/Mo.

3.2. Electroacoustic properties of AlScN films

As described in Paper IV, FBAR devices were fabricated in order to investigate the electroacoustic properties of $Al_{(1-x)}Sc_xN$ films. The results presented and discussed here refer to the compositions x = 0, 0.03, 0.09 and 0.15.

The θ-2θ XRD scans of all four film compositions are presented in *Figure 13*. The value of the FWHM extracted from the rocking curve of each film is indicated in *Figure 13* as well. The well aligned (002) peak, the low values of FWHM and the absence of other AlN crystal orientations indicate that the $Al_{(1-x)}Sc_xN$ films are highly textured and c-axis oriented. The peaks at 38.5° and 40.5° are related to the metals used as bottom and top electrodes: Mo (110) and Al (111), respectively. It can be noted also at *Figure 13* a slight downshift of the (002) peak at the compositions x = 0.09 and 0.15. This is due to the residual stress[17], which is more pronounced at the films with higher Sc concentration. Most likely, this behavior is caused by the increase in the lattice mismatch between the film and the substrate by adding higher amounts of Sc in the $Al_{(1-x)}Sc_xN$ films.

The measurements for the electroacoustic characterization were performed in a network analyzer (standard configuration) and the wave excitation mode was the longitudinal[18] one. The equipment was calibrated for a 50 Ohm input impedance and central frequency around the central resonance frequency of the fabricated FBARs (2.35 MHz).

In order to extract the electrical and acoustic parameters of $Al_{(1-x)}Sc_xN$ films, the measured data were fitted to the Modified Butterworth Van-Dyke[19] (MBVD) and one-dimensional Nowotny-Benes[20] (NB) models by using the software ADS® (Agilent Technologies) . The procedure is described in detail in Paper IV (item 3).

The doping of AlN films with Sc leads to a softening of the material, i.e., the $Al_{(1-x)}Sc_xN$ films become softer as the Sc concentration increases. This phenomenon has an impact on the electroacoustic properties of the film, clearly evidenced by the reduction of the quality factor (Q-factor) as indicated in *Figure 14*. Even though the films become softer their piezoelectric properties are enhanced, which leads to an improvement of the coupling coefficient (refer to *Figure 14*). Noteworthy, the coupling coefficient was increased by 100% when comparing pure AlN films and $Al_{(1-}$

[17] The deposition conditions are the major reasons for the appearance of residual stress in thin films (substrate temperature, input power and gas pressure, for instance). The direction (compressive or tensile) and magnitude of the residual stress are mostly influenced by the deposition conditions. Noteworthy, the thickness of the thin film can also influence this parameter [16, 18, 36, 66].

[18] In the longitudinal wave propagation mode, the direction of particle motion is parallel to the direction of the wave propagation (see *Figure 2*).

[19] For further information and references about this model, see Paper IV.

[20] Idem.

$_{x)}Sc_xN$ with the highest Sc concentration (x = 0.15) used in the fabricated FBAR devices.

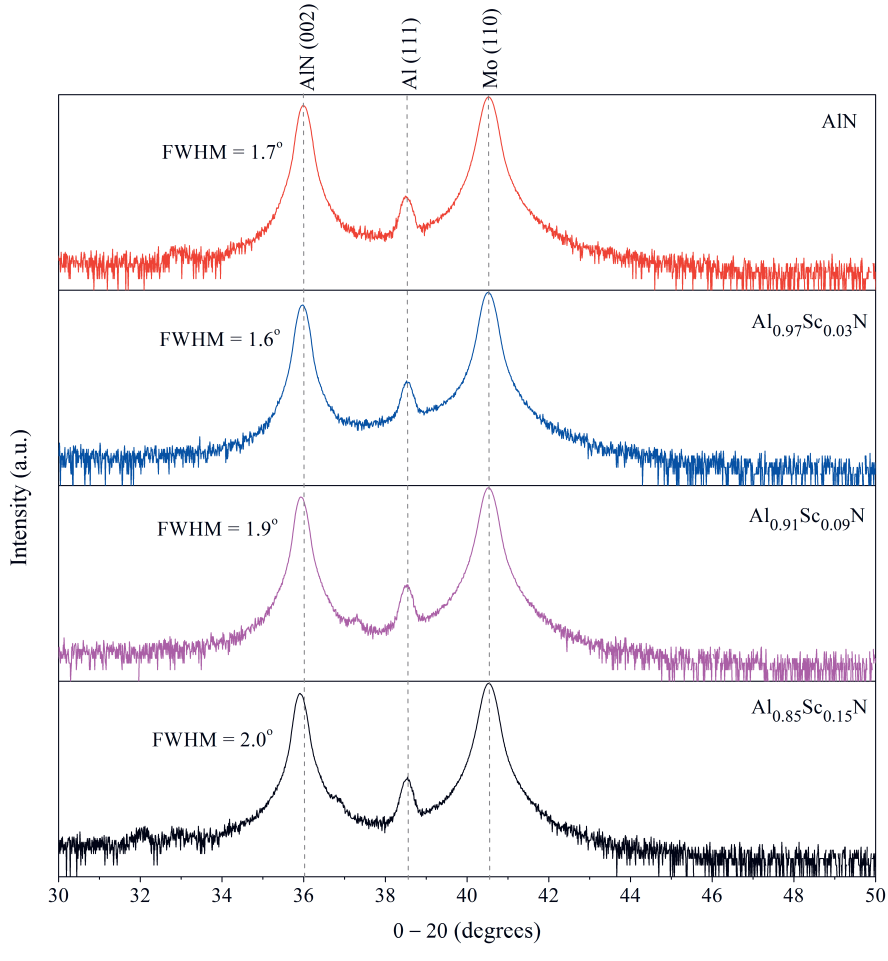

Figure 13. θ-2θ scans of $Al_{(1-x)}Sc_xN$ films of the FBAR devices (x = 0, 0.03, 0.09 and 0.15).

Therefore, there is a tradeoff to be evaluated when doping AlN films with Sc: increase the coupling coefficient and improve the efficiency to which the piezoelectric material will convert electrical into mechanical energy (and vice-versa); or keep the quality factor as high as possible, ergo lowering the energy dissipation? Thus, the Figure of Merit (FOM) can be used as an indicator of the optimal compromising relationship. In the case of electroacoustic devices, the FOM is defined as the product k_t^2 x Q. Based on the measured values $k^2_{eff,m}$ and $Q_{B,m}$, the FOM was calculated for each $Al_{(1-x)}Sc_xN$ composition, and the maximum FOM achieved was 65.55 for the film with 9% of Sc (see *Figure 15*).

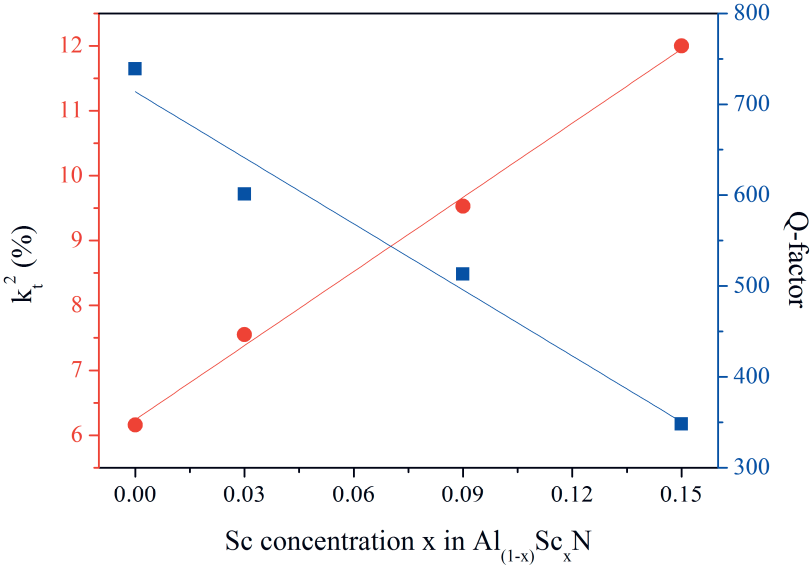

Figure 14. Electromechanical coupling (k_t^2) and quality factor (Q-factor) as a function of the Sc concentration in $Al_{(1-x)}Sc_xN$ films.

The temperature coefficient of frequency (TCF[21]) is also an important parameter to investigate in order to evaluate the performance of the devices operating at higher temperatures. To this end, the FBARs were heated in the temperature interval 25 - 125 ^oC and their resonance frequencies were re-measured. The results are presented in *Figure 16*. It can be noted that the TCF tends to increase with the Sc concentration in the films. A possible solution to this issue is the use of a compensating layer of SiO_2 in the FBAR structure. The SiO_2 has a positive temperature coefficient of frequency and it has been largely used as a thermal compensating layer in resonators operating at high temperatures [67-69].

[21] The TCF indicates the relative change of the resonance frequency with the change of temperature. It is desirable to have this coefficient as near to zero as possible.

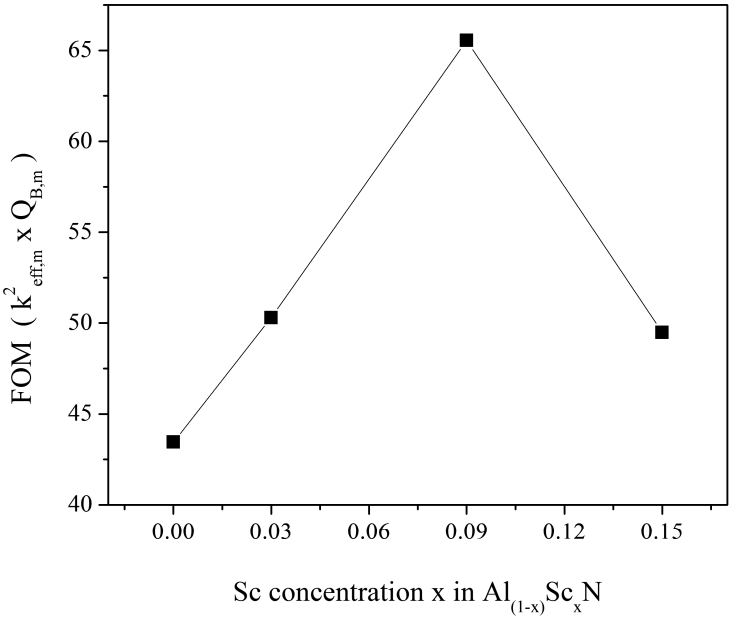

Figure 15. Figure of merit (FOM) calculated for FBAR devices based on $Al_{(1-x)}Sc_xN$ and Sc concentration of 0, 3, 9 and 15%.

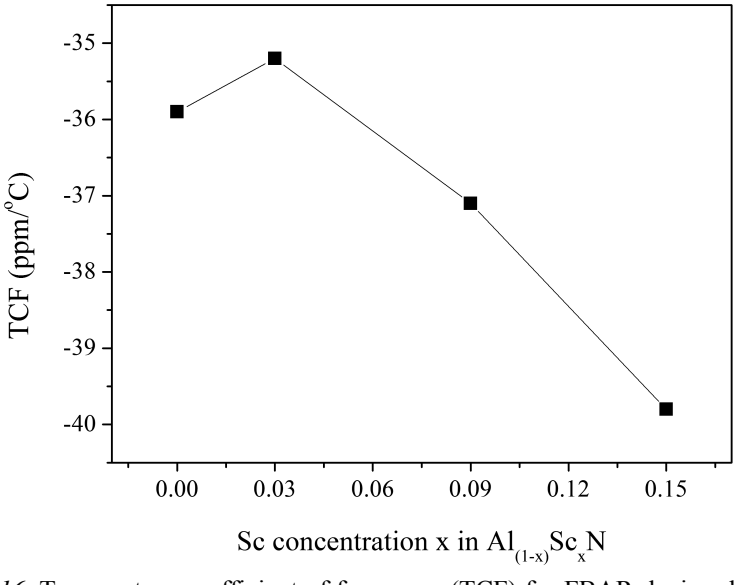

Figure 16. Temperature coefficient of frequency (TCF) for FBAR devices based on $Al_{(1-x)}Sc_xN$ and Sc concentrations of 0, 3, 9 and 15%.

In addition to the acoustic properties studies, the electric parameters ε_r and tan δ[22] were investigated in order to evaluate the electrical behavior of $Al_{(1-x)}Sc_xN$ films as a function of the Sc concentration. The relative dielectric permittivity, ε_r, was calculated from the extracted static capacitance of the fabricated FBARs (see Paper IV, item 3). Metal-insulator-metal (MIM) capacitors were fabricated to extract the dielectric losses, tan δ. These results are shown in *Figure 17*.

It can be noted an undesirable increase in the tan δ parameter by increasing the amount of Sc in the films. However, these values are still lower (or similar to) when comparing with other concurrent piezoelectric materials, such as ZnO and PZT [70, 71].

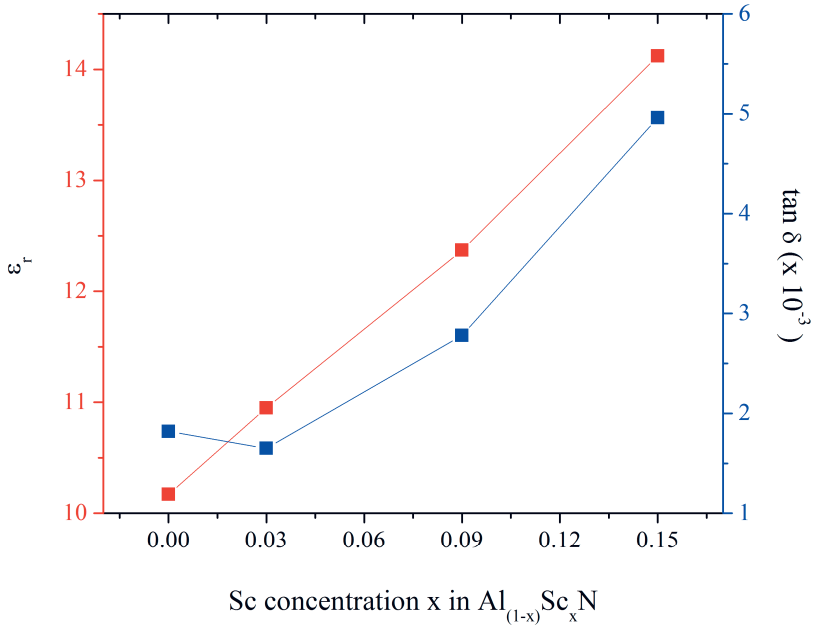

Figure 17. Dielectric permittivity, ε_r, and dielectric losses, tan δ, as a function of the Sc concentration in $Al_{(1-x)}Sc_xN$ films.

3.3. HiPIMS and AlN films

It was already mentioned before that different parameters and conditions can influence the final texture of sputtered AlN films. Substrate material, deposition temperature, target power, pressure, gas flows and target-to-substrate distance are some of them. However, not least important is the

[22] The dielectric loss, tan δ, quantify the energy loss (heat) inherent to a dielectric material and it is calculated in here by the ratio imaginary/real part of the dielectric constant.

condition of the nucleation layer of the films. More commonly, attention has been given in the literature to the growth of suitable nucleation layers when c-axis tilted AlN films are studied. In this case, the nucleation layer should be poor in (002) crystal orientations. Notwithstanding, a nucleation layer rich in (002) crystal planes is the best choice in order to grow c-axis textured AlN films.

At the work presented in Paper I, different deposition conditions were tested using the HiPIMS method and aiming the improvement of the nucleation layer properties of AlN films. Furthermore, depositions by conventional Pulsed DC (under similar conditions as the depositions done by HiPIMS) were performed for comparative studies. Since the use of a bottom electrode is required for certain devices applications, the analysis should be extended to AlN films deposited on top of metal layers as well. Thus, all films were deposited onto two different substrates: Si and textured Mo. The reasons why Mo was chosen as the metal layer and its use in the textured composition were previously presented (see item 3.1). XRD measurements were performed in order to evaluate the film properties (more specifically, θ-2θ scans and FWHM of the rocking curve).

Some authors consider that below certain N_2 flow levels, there is not enough N_2 to grow AlN. On the other hand, above certain N_2 levels there are not enough Al atoms [14]. Clearly there is an optimal range of gas flows in within which the N_2 flow is suitable to the growth of stoichiometric c-axis oriented AlN films. Obviously this range is not the same for all experimental setups, varying from machine to machine and, furthermore, varying with other deposition conditions.

Thus, in order to identify the optimal gas composition Ar/N_2 for the HiPIMS, different gas flows were used for AlN depositions on both types of substrates (Si and textured Mo). The total flow was kept constant at 70 sccm and four different compositions were tested (Ar/N_2, in sccm): (i) 30/40, (ii) 35/35, (iii) 40/30 and (iv) 45/25.

One can see in *Figure 18b* that all gas compositions tested were favorable to the growth of AlN (002) on top of textured Mo layers. However, an undesirable AlN (103) is noted on the films deposited by the composition Ar/N_2 30/40 sccm.

In the case of films deposited directly on Si, the AlN (002) peak is totally vanished at 45/25 sccm gas flows and shows the lowest intensity at 40/30 sccm composition (*Figure 18a*).

Thus, based on the above observations, the composition 35/35 sccm was chosen as the optimal gas flows ratio. Noteworthy, at this gas composition the AlN (103) peak has the lowest intensity for the films deposited on Si substrates by the HiPIMS technique.

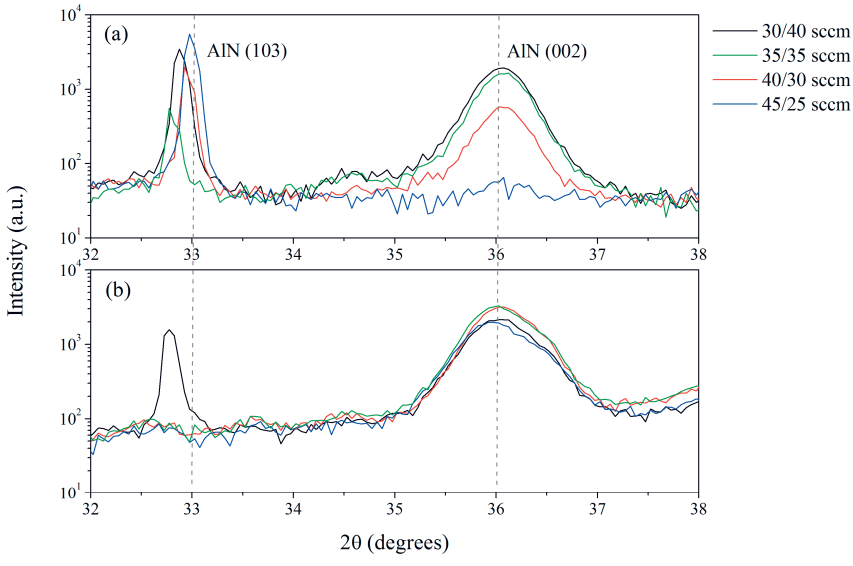

Figure 18. θ-2θ scans of AlN films deposited by HiPIMS at room temperature and different gas flows ratio (Ar/N_2) on top of (a) Si substrates and (b) textured Mo substrates.

Considering that the c-axis texture is improved by the substrate temperature at Pulsed DC depositions, the study of this phenomenon was shortly investigated for the HiPIMS depositions as well. Nevertheless, the influence of the temperature was not the main focus of the investigation. Thus, only three substrate temperatures were tested: room temperature, 300 ^{o}C and 400 ^{o}C. The optimal gas flow composition was used (35/35 sccm) and the films were deposited on both types of substrates. The results are shown in *Figure 19*.

Even though the AlN (002) peak is very similar for the films deposited at 300 ^{o}C and at 400 ^{o}C on textured Mo, the peak intensity is slightly higher for the film deposited at 400 ^{o}C on Si substrates. Thus, 400 ^{o}C was chosen as the deposition temperature for the comparative studies. It is important to reinforce in here that the temperature analysis was not the focus of the work, ergo the analysis of its effects on the HiPIMS depositions was marginal.

By knowing the optimal conditions for the growth of textured AlN films by means of HiPIMS method, the next step in the studies was the comparison of the films deposited by HiPIMS and Pulsed DC techniques. As showed in *Figure 20* and *Figure 21*, it is clear the improvement in the AlN films brought by the HiPIMS method. Most likely, this is due to the higher degree of ionization (high plasma density) during the HiPIMS depositions, which in turns provides an enhancement in the adatoms mobility at the

surface during the film growth. Noteworthy, the films were deposited under similar conditions (refer to Paper I for more details).

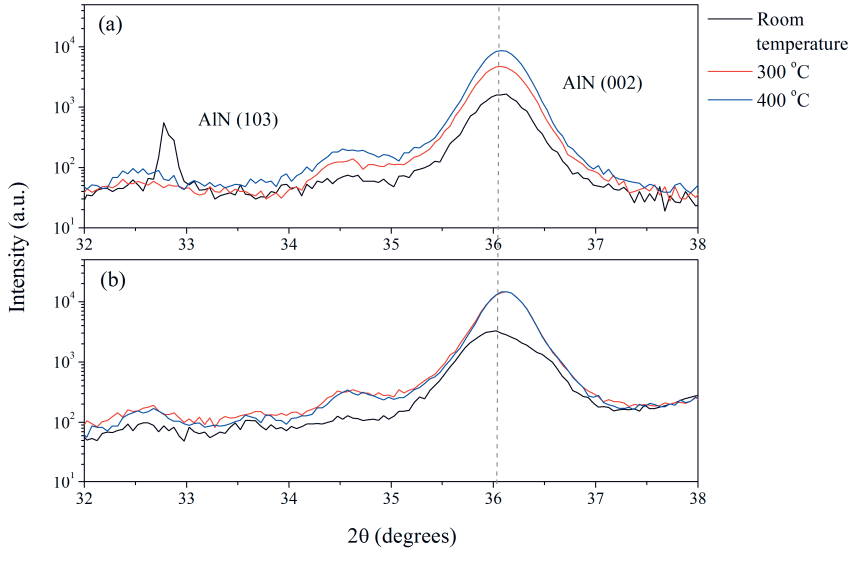

Figure 19. θ-2θ scans of AlN films deposited by HiPIMS at fixed gas flow ratio (Ar/N_2 35/35 sccm) and different deposition temperatures on top of (a) Si substrates and (b) textured Mo substrates.

The results in *Figure 20a* show that at room temperature and by means of Pulsed DC depositions it was not possible to grow AlN (002) films on Si, even at different gas flows. On the other hand, even if followed by an undesirable (103) peak, the HiPIMS film shows a well pronounced (002) peak.

Since the results are quite poor for the Pulsed DC films deposited at room temperature, it was not possible to define the optimal gas flow composition. Thus, the 35/35 sccm was chosen as the gas flow for the comparison of HiPIMS and Pulsed DC deposited at higher temperature (400 ^{o}C). As expected, the quality of both films is improved by the temperature (see *Figure 20b*). However, the HiPIMS film exceeds the Pulsed DC. Moreover, the AlN (103) peak found at the room temperature deposition was vanished for the HiPIMS at 400 ^{o}C.

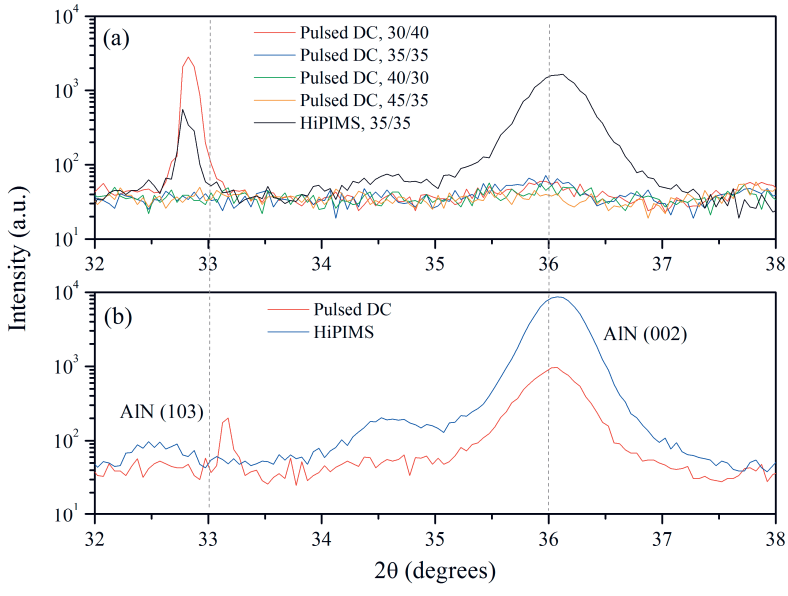

Figure 20. θ-2θ scans of AlN films deposited by Pulsed DC and HiPIMS on Si substrates: (a) at room temperature and different gas compositions for the Pulsed DC films; (b) at 400 ^{o}C and Ar/N_2 35/35 sccm as gas flow composition.

It is important to point out here that these results refer to a certain experimental setup. It doesn't mean the AlN films deposited by Pulsed DC at room temperature and on top of Si substrates will present the same poor results for all experimental setups. However, it is also important to point out that this is a comparative study, and the films were deposited under similar conditions (same target-to-substrate distance, similar base and deposition pressures, and so on). In our understanding this means that, by changing the experimental setup and keeping the deposition conditions similar for both techniques, HiPIMS will continue showing an improvement in the AlN films characteristics in comparison with the Pulsed DC ones.

As can be seen in *Figure 21*, there were no pronounced differences between the films growth by both deposition methods on textured Mo substrates at room temperature (*Figure 21a*) or at 400 ^{o}C (gas composition 35/35 sccm, *Figure 21b*). One can consider that the textured Mo layer is already the optimal seed layer for the AlN films. Thus, in this case the deposition method does not influence so strongly the film growth (as long as it provides enough kinetic energy to the atoms).

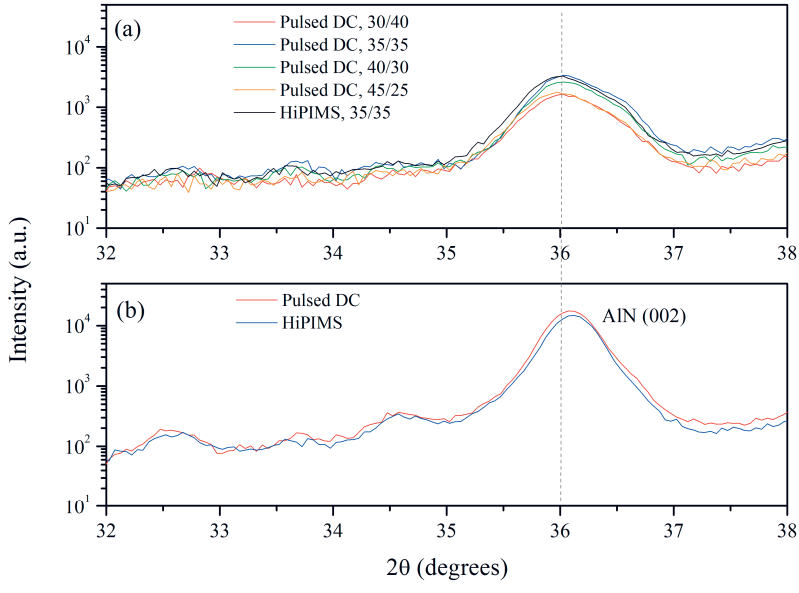

Figure 21. θ-2θ scans of AlN films deposited by Pulsed DC and HiPIMS on textured Mo layers: (a) at room temperature and different gas compositions for the Pulsed DC films; (b) at 400 ^{o}C and Ar/N_2 35/35 sccm as gas flow composition.

The beneficial effect of the HiPIMS method on the texture of the AlN films is seen in *Figure 22*. The FWHM of the (002) rocking curves presented refer to the films deposited at the gas composition Ar/N_2 35/35 sccm. There is no FWHM for the AlN films sputtered by Pulsed DC on Si substrates and at room temperature since the (002) peak was vanished at this deposition condition (refer to *Figure 20*).

One can say that the HiPIMS method can be considered as a promising technique to deposit suitable nucleation layers for the growth of c-axis textured AlN films.

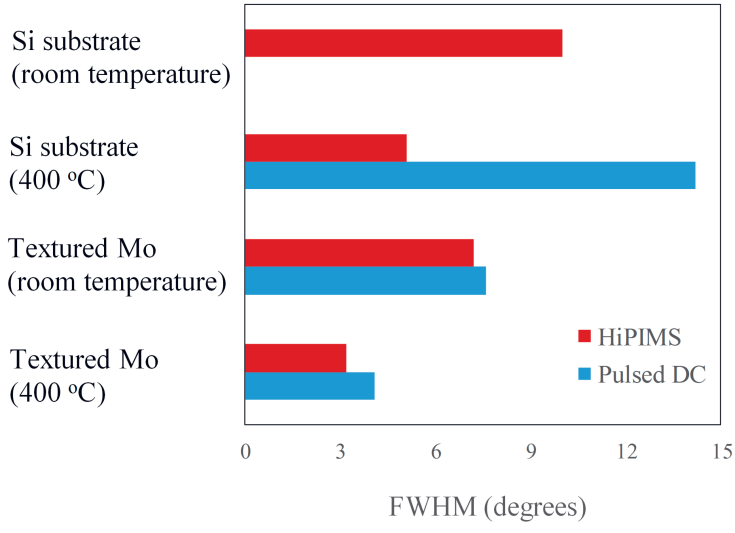

Figure 22. FWHM of AlN films deposited by Pulsed DC and HiPIMS on Si and textured Mo substrates, at room temperature and 400 ºC.

Chapter 4. Summary of included papers

4.1. Paper I: Thin AlN films deposited by reactive HiPIMS and Pulsed DC sputtering: a comparative study

Manuscript to be submitted.

Author's contribution: Part of planning and analysis. Major part of thin films deposition (Pulsed DC and HiPIMS) and measurements. Significant part of writing.

The motivation of this work was the deposition of textured (002) AlN thin layers directly on Si substrates, at reduced temperatures and in a setup with long target-to-substrate distance. It can be difficult to growth textured films by means of conventional Pulsed DC depositions when these three conditions are combined. For instance, in order to grow texture AlN by Pulsed DC, higher deposition temperatures are applied to compensate the long target-to-substrate distance, or suitable seed layers to the growth of (002) AlN films (such as Mo, Pt, Au) need to be used.

Thus, thin AlN films (200 nm) were deposited by HiPIMS and Pulsed DC under similar conditions and the results were compared. The depositions were performed at the same experimental setup, and the power supply was the single physical change between both processes. The deposition conditions are summarized in *Table 3*.

Table 3. Summary of the deposition conditions of HiPIMS and conventional Pulsed DC.

	Pulsed DC	**HiPIMS**
Pressure	2.8 – 3.2 mTorr	
Pre-sputtering time (in pure Ar)	3 min	
Pre-sputtering power	200 W	400 W
Discharge power	800 W	830 W
Pulse frequency	250 KHz	1 KHz
Duty cycle	12.5%	5%

The gas flow ratio Ar/N_2 was optimized for the HiPIMS process. Supported by θ-2θ scans (X-ray diffraction analysis), the films deposited at 35/35 sccm presented the best results. Thus, this gas composition was used for both deposition processes (HiPIMS and Pulsed DC).

In order to evaluate the influence of the substrate material, besides the depositions directly on Si, AlN films were also grown on top of textured Mo layers. Furthermore, the influence of the deposition temperature was also analyzed.

Noteworthy, samples deposited by a standard deposition process were used as reference samples. This standard process is performed by Pulsed DC sputtering in a system with short target-to-substrate distance, which is favorable to the growth of textured films. It should be noted that the deposition conditions were similar to those presented in *Table 3* for the Pulsed DC process.

The results indicate a substantial improvement brought by the HiPIMS method over the Pulsed DC ones. Notably, the texture of the AlN films deposited by HiPIMS excels the Pulsed DC process for the samples deposited on Si and at room temperature.

Therefore, it was demonstrated the possibility to obtain textured (002) AlN films deposited on Si substrates, at reduced temperatures and in systems with long target-to-substrate distances by means of HiPIMS depositions.

4.2. Paper II: Efficient RF voltage transformer with bandpass filter characteristics

M. Moreira, J. Bjurström, I. Katardjiev, and V. Yantchev, "Efficient RF voltage transformer with bandpass filter characteristics," *Electronics Letters,* vol. 49, pp. 198-199, 2013.

Author's contribution: Minor part of planning. Involved in fabrication and measurements. Minor writing.

The main objective of this work is to develop a realistic solution to a passive, addressable, remotely controlled switch using far field communication. By definition, such switches make use of the energy of the control signal the power of which decays exponentially with distance in addition to being limited by existing RF emission regulations. This necessitates both power accumulation and voltage amplification in order to generate a usable DC signal for switching. Further, addressability requires frequency modulation which necessitates the use of bandpass filters. All these requirements make existing solutions totally impractical in terms of both performance and cost. The solution proposed addresses elegantly both of these aspects by

developing a single component with a dual functionality, that is, it is both a highly efficient voltage transformer and a bandpass filter at the same time. Called transfilter for brevity, the device represents an electroacoustic bandpass filter with a large input/output impedance ratio (transformer characteristic).

The transfilter designed is a 2-port Lamb wave resonator using a highly c-axis oriented AlN piezoelectric thin film. Input and output are realized by interdigital transducers (IDT) and energy confinement is achieved by the use of reflectors with the same pitch as the IDT (see *Figure 23*). Whereas the resonance frequency of the transfilter is defined by the pitch of the IDT, devices with different resonance frequencies can be fabricated on a single chip having a common input and distinct outputs.

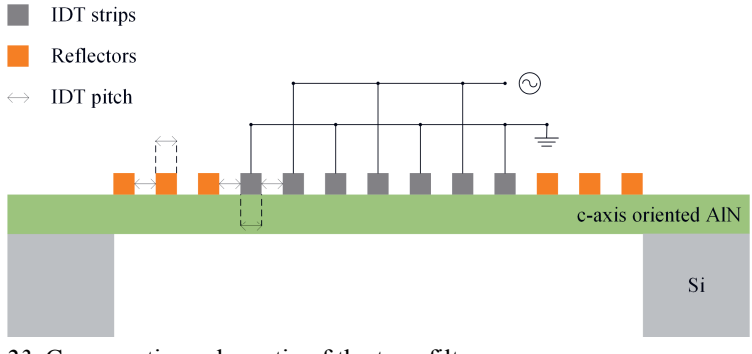

Figure 23. Cross section schematic of the transfilter.

The transfilter was fabricated (*Figure 24*) using standard planar technology and was electrically characterized around its resonance frequency (888 MHz) by a Network Analyzer. Under open circuit conditions, an AC voltage input of 0.2 V was applied, returning a voltage output of approximately 2 V, thereby confirming the voltage amplification of the input signal. This voltage transformer ratio can be varied in a wide range by varying the ratio between input and output impedances (varying the number of pairs of the input and output IDT).

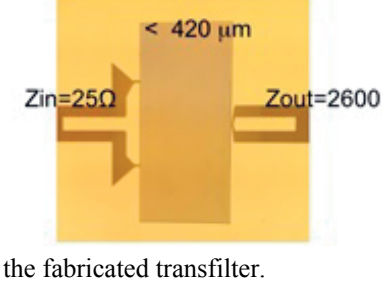

Figure 24. Top view of the fabricated transfilter.

By the use of transfilters, truly passive and addressable RTS can be built by employing capacitive MEMS switches (*Figure 25*).

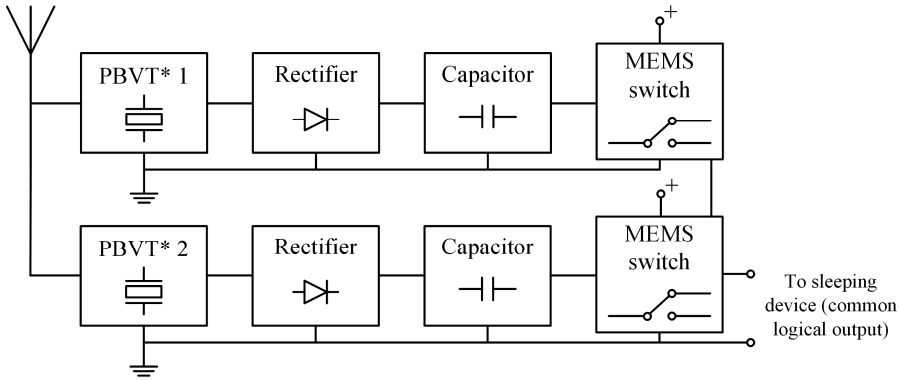

Figure 25. Schematic of a truly passive and addressable RTS by the use of transfilters (*PBVT: see footnote).

In comparison with existing commercial wireless technologies (notably RFID tags), the obvious advantages of the transfilter are (i) quite low internal energy accumulation in the device, (ii) it is a linear device, it operates at all input power levels, i.e. no threshold, (iii) low cost and size and (iv) high efficiency. As a stand-alone component it can also be used in efficient AC/DC charge pumps.

Noteworthy, the design of the transfilter is not solely confined to Lamb wave devices and AlN thin films. Analogously, similar or even better performances can be obtained by using other piezolelectric materials and acoustic waves. Specifically, an insertion loss of -1 dB in the passband is quite feasible with today's filter design technologies, making the transfilter an extremely efficient component unrivalled by existing solutions.

4.3. Paper III: Preparation and characterization of high-k aluminium nitride (AlN) thin film for sensor and integrated circuits applications

J. F. Souza, M. A. Moreira, I. Doi, J. A. Diniz, P. J. Tatsch, and J. L. Gonçalves, "Preparation and characterization of high-k aluminium nitride (AlN) thin film for sensor and integrated circuits applications," *Physica Status Solidi (c),* vol. 9, pp. 1454-1457, 2012.

*PBVT: piezoelectric bandpass voltage transformer

Author's contribution: Minor part of planning. Major part of synthesis and characterization of AlN for the application as the transistor gate. Minor writing.

There a continuous trend to downsize scaling of transistor based devices (MISFET and ISFET, for instance)[23]. To this end, all layers and dimensions of these devices should follow the same trend. However, there are some limitations related with the materials properties. For example, SiO_2 is the most common used material as gate dielectric and the downsizing of its thickness implies in an increasing of the leakage current through it. Therefore, this downsize scaling has been driving the research efforts to find dielectric materials with high-k to replace the SiO_2 as gate dielectric while keeping (or improving) the performance of the device.

This paper reports the use of AlN films as gate dielectric for MISFETs and ion sensitive membrane for EISFETs devices.

The sputtered AlN films were prior synthesized in order to reach the desirable characteristics (polycrystalline, c-axis oriented, smooth surface and stoichiometric films). The devices were fabricated following the standard transistors fabrication process. The thickness of the AlN films deposited is 30 nm. A thin layer of SiO_2 (5 nm) was stacked to the AlN layer in order to reduce the mobile charges in the interface dielectric-semiconductor.

C-V measurements were done with the aim of determine the electrical quality of the AlN/SiO_2 stacked layer and $AlN/SiO_2/Si(100)$ interface. These measurements were performed at the MIS capacitor intrinsic to the MISFET device (see *Figure 26*). The results (see *Table 4*) confirm that the AlN/SiO_2 stacked layer is a good insulator on silicon substrates.

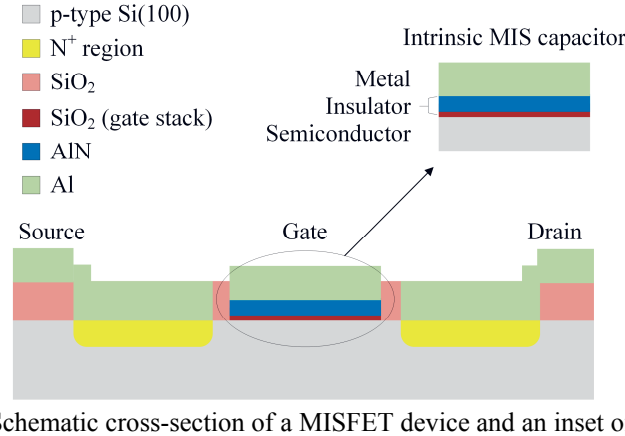

Figure 26. Schematic cross-section of a MISFET device and an inset of its intrinsic MIS capacitor.

[23] According to the Moore's law, the amount of transistors in an integrated circuit double around every two years.

Table 4. Electrical parameters (measured and calculated) of the AlN/SiO_2 stacked layer.

Maximum capacitance C_{max}	158.5 pF
Minimum capacitance C_{min}	40.66 pF
Substrate acceptor concentration N_A	1.87×10^{17} cm^{-3}
Flat-band capacitance C_{fb}	116.71 pF
Equivalent oxide thickness EOT	8.71 nm
Flat-band voltage V_{fb}	-0.59 V
Work function metal-semiconductor ϕ_{ms}	-1.02 V
Charge trap density (negative) N_t	-1.02×10^{12} cm^{-2}
Threshold voltage V_{th}	0.84 V

Furthermore, the MISFET and EISFET[24] devices were electrically characterized by means of their $I_{DS}xV_{GS}$ curves. The calculated values are summarized in *Table 5*.

Table 5. Electrical parameters of MISFET and EISFET devices.

	MISFET	**EISFET**
Transconductance G_m	96 µs	329 µs
Current-off I_{off}	5×10^{-11} A	1.88×10^{-9} A
Subthreshold swing S_t	103 mV/dec	171 mV/dec

The possibility to use AlN as gate insulator in MISFET and EISFET devices was demonstrated by fabricating and characterizing such devices.

4.4. Paper IV: Aluminum scandium nitride thin-film bulk acoustic resonators for wide band applications

M. Moreira, J. Bjurström, I. Katardjiev, and V. Yantchev, "Aluminum scandium nitride thin-film bulk acoustic resonators for wide band applications," *Vacuum,* vol. 86, pp. 23-26, 2011.

Author's contribution: Part of planning. Involved in synthesis and characterization of AlScN films. Involved in fabrication and characterization of FBARs. Minor writing.

[24] A standard pH 7 solution was used for the EISFET measurements.

This paper is the first to present an experimental electroacoustic characterization of highly c-textured $Al_{(1-x)}Sc_xN$ piezoelectric films as a function of Sc concentration in view of wide band telecom applications in the low GHz range. For this purpose, one port FBAR test devices were fabricated with four different Sc concentrations, namely x = 0, 0.03, 0.09 and 0.15 respectively. The films were grown by reactive sputter deposition under identical conditions as illustrated in *Table 6*.

Table 6. Deposition conditions of the $Al_{(1-x)}Sc_xN$ layers.

Base pressure	$< 2 \times 10^{-8}$ Torr
Deposition pressure	2.8 mTorr
Substrate temperature	400 °C
Ar flow	30 sccm
N_2 flow	30 sccm

In order to obtain films with a high crystallographic texture a double seed layer consisting of a 120 nm thick (002) AlN layer and a 300 nm thick (110) textured Mo layer was used. The high c-axis texture of the $Al_{(1-x)}Sc_xN$ films was confirmed by X-ray diffraction analysis. The XRD measurements showed that all films are c-axis oriented and highly textured, with a FWHM of the (002) peaks varying from 1.6° up to 2° with increasing Sc concentration.

A simplified cross-section of the FBAR structure is shown in *Figure 27*.

Figure 27. Cross-section view of the resonator structure.

The electroacoustic characterization of the FBARs was performed with a network analyzer and the scattering parameters were acquired at frequencies around the fundamental longitudinal resonance of each device. It is noted that a slight downshift of the resonance frequency with increasing the Sc concentration was observed.

The measured data were fitted to the MBVD equivalent circuit, which yielded a negligible shunt resistance (R_0) and a series parasitic resistance

(R_s) of around 0.3 Ohms for all resonators. The unknown stiffness C_{33} and piezoelectric constant e_{33} parameters were determined by a combination of the one-dimensional Nowotny-Benes model and the MBVD extraction. Both parameters were varied to best fit the series resonance frequency f_s and the effective electromechanical coupling k_{eff}^2 from the MBVD extraction. The relative dielectric permittivity ε_r was extracted from the static FBAR capacitance C_0.

Other parameters such as the parallel resonance (f_p), the Q-factor at parallel resonance (Q_p) and the unloaded Q-factor (Q_B) were obtained from the electroacoustic measurements.

Table 7 shows the most relevant parameters measured/extracted, including the intrinsic electromechanical coupling k_t^2 for all four different Sc concentrations.

Table 7. Measured and extracted $Al_{(1-x)}Sc_xN$ parameters.

Composition	**f_s (GHz)**	**Q_B**	**k_{eff}^2 (%)**	**FOM**	**ε_r**	**C_{33} (GPa)**	**e_{33} (C/m^2)**	**k_t^2 (%)**
AlN	2.3605	790	5.50	40	10.1	370	1.48	6.16
$Al_{0.97}Sc_{0.03}N$	2.2935	730	6.89	50	10.9	346	1.66	7.55
$Al_{0.91}Sc_{0.09}N$	2.2339	690	9.50	65	12.4	326	1.94	9.53
$Al_{0.85}Sc_{0.15}N$	2.1522	410	12.07	60	14.1	270	2.14	12.00

It is seen in *Table 7* that the electromechanical coupling increases steadily with increasing Sc concentration to exceed by 100% that of pure AlN at a Sc concentration of x = 0.15. In other words, the latter films may be used for the fabrication of bandpass filters with a twice as large bandwidth than that of pure AlN. Another important finding is that the Q-value correspondingly decreases with increasing Sc concentration owing to increased acoustic losses associated with a correspondingly increased softness of the films as manifested by the decrease in the C_{33} elastic constant.

However, more important for filter design is the FOM defined as the product between the electromechanical coupling and the Q value. As seen in *Table 7* this FOM exhibits a maximum for x = 0.09.

The above results demonstrate unequivocally that highly textured $Al_{(1-x)}Sc_xN$ films can be used for the fabrication of high performance telecom components with a large bandwidth.

4.5. Paper V: Synthesis of c-tilted AlN films with a good tilt and thickness uniformity

M. Moreira, J. Bjurström, T. Kubart, B. Kuzavas, and I. Katardjiev, "Synthesis of c-tilted AlN films with a good tilt and thickness uniformity," in *IEEE International Ultrasonics Symposium Proceedings*, 2011, pp. 1238-1241.

Author's contribution: Minor part of planning. Involved in thin films depositions and measurements. Minor writing.

AlN films with a nonzero tilt of the c-axis have been studied for use in electroacoustic devices in the shear thickness propagation mode (see *Figure 28*) operating in liquid media. In the latter case propagation of the shear mode is confined to the resonating cavity (piezoelectric layer including electrodes), since shear motion is not supported in liquid media and hence the resonator retains its high Q-factor. Certain degradation of Q is inevitable due to viscous loading from the liquid but the overall Q-value is still sufficiently high to guarantee low noise performance. In terms of biosensor applications, for instance, this leads to a higher mass and viscosity resolution.

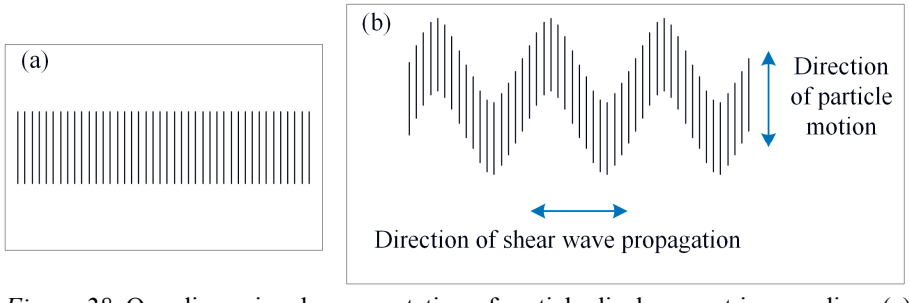

Figure 28. One dimensional representation of particle displacement in a medium (a) without any wave motion, and (b) with shear thickness wave propagation.

This paper describes a method for the deposition of c-tilted AlN films by pulsed DC sputtering with good uniformity of both tilt and thickness throughout the wafer. Other existing methods for the deposition of c-tilted AlN films suffer from serious drawbacks such as low deposition rates and non-uniform thickness and tilt. In this sense, the method presented here intends to overcome these shortcomings. To this end, it is primordial to have an adequate handle on both the nucleation and the growth stages. The strategy of the method presented here is as follows. During nucleation, optimal conditions are chosen which hamper the nucleation of grains with the c-plane parallel to the surface and instead promote nucleation of a sizable

population of grains with a crystallographic orientation non-parallel to the average film surface. During the growth stage, optimal conditions are chosen which promote the growth of non c-oriented grains whose c-axis lies in a specific half-plane perpendicular to the film surface. Growth of grains with other crystallographic orientations is suppressed. In this way, a film with a monodirectional tilt of the c-axis is obtained. This growth stage is typically achieved by assuring a certain directionality of the deposition flux, say by operating the process at relatively low pressures which minimizes scattering in the gas phase.

A suitable nucleation layer for tilted AlN growth can be achieved by: (i) rough substrate surface and/or (ii) crystallographic mismatch between substrate and the film (non-hexagonal structure in case of AlN films) and/or (iii) a non-textured AlN seed layer, which can be obtained under diffusion limited nucleation conditions, e.g., at high deposition pressures and low substrate temperatures.

The growth of tilted films proposed in this paper suggests the use of an array of linear magnetrons instead of the conventional magnetrons with circular symmetry (see *Figure 29*).

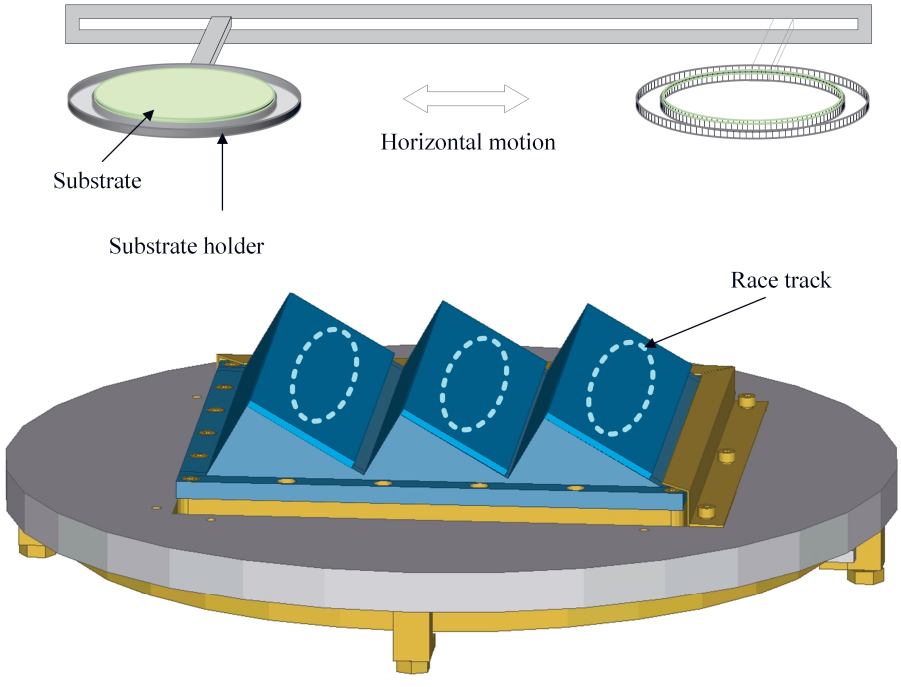

Figure 29. Array of tilted magnetrons.

Assuming that the majority of the sputtered atoms arrive at the substrate at angles close to the surface normal, the tilt of the magnetron segments relative to the surface normal sets the incident angle of the deposition flux.

However, it is also necessary to achieve thickness uniformity. To this end, the substrate is moved horizontally along the projection of the atoms flux from the target towards the substrate (refer to *Figure 29*).

XRD pole plot figures clearly demonstrate the significant improvement in the tilt distribution resulting from the magnetron array proposed (see *Figure 30*). Even though a c-tilted film was previously demonstrated by conventional magnetron deposition (*Figure 30a*), it exhibited a broad tilt distribution as indicated by the kidney shape of the XRD pole plot. On the other hand, the narrower tilt distribution of the film deposited by the use of the magnetron array shows that a higher texture was attained (*Figure 30b*).

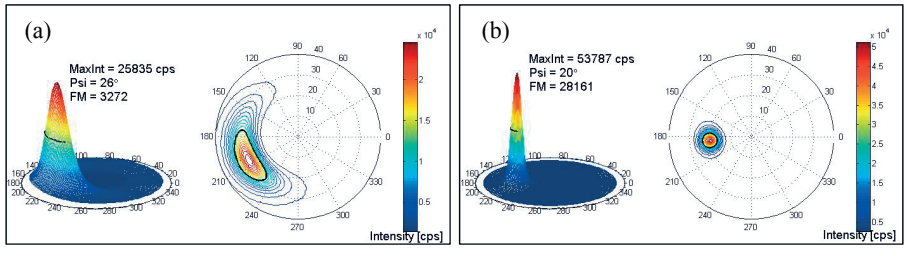

Figure 30. XRD pole plot figures of tilted AlN films deposited by use of (a) a conventional magnetron with circular symmetry and (b) an array of tilted magnetrons.

It is likely that the use of the array of linear magnetrons in addition to an adequate control of the nucleation stage are suitable to the growth of not only tilted AlN films, but other wurtzite thin films as well.

4.6. Paper VI: Electrical characterization and morphological properties of AlN films prepared by dc reactive magnetron sputtering

M. A. Moreira, I. Doi, J. F. Souza, and J. A. Diniz, "Electrical characterization and morphological properties of AlN films prepared by dc reactive magnetron sputtering," *Microelectronic Engineering,* vol. 88, pp. 802-806, 2011.

Author's contribution: Part of planning. All fabrication and measurements. Significant part of writing.

The paper describes the physical and electrical characterization of sputtered AlN films deposited by different conditions. Notwithstanding AlN is a well-known material and the influence of the deposition conditions on its quality have been presented in the literature by other groups, there is still a lack of

results regarding it. In this sense, more studies will contribute in the further development of high quality AlN thin films.

The deposition conditions that changed in this paper were N_2 flow ratio and discharge power. The physical parameters analyzed were roughness, crystallographic texture, absorbance, resistivity and refractive index. In addition, electrical parameters were analyzed such as dielectric constant, hysteresis, equivalent oxide thickness and flat band voltage. To this latter end, Metal-Insulator-Semiconductor (MIS) capacitors were fabricated (*Figure 31*) and some of them where annealed. Therefore, the electrical parameters were studied not only as a function of N_2 flow and target power, but also as a function of insulator thickness and heat treatment of the MIS structures.

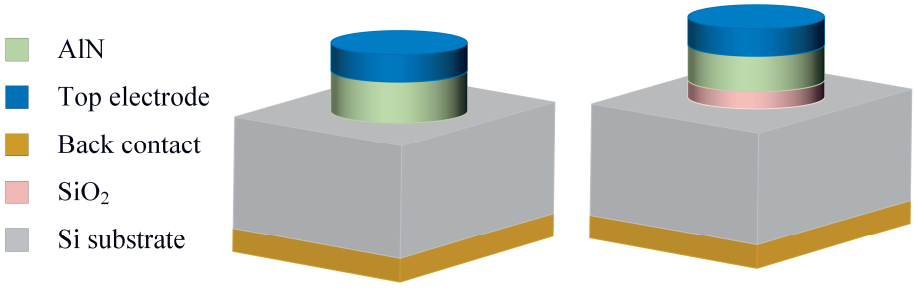

Figure 31. Schematic of the MIS capacitors fabricated.

The achieved results showed the formation of reasonably good AlN thin films, applicable in some electronic devices. The equipment used to deposit those films was not fully explored yet and it has a great potential to develop uniform and highly textured films (short target-to-substrate distance and large targets, for instance).

Chapter 5. Concluding remarks

The intrinsic properties of AlN make it an outstanding material among other piezoelectric materials. It can be used in a wide variety of applications such as:

- Microelectromechanical systems,
- Electroacoustic sensors (including biosensors),
- High frequency filters and oscillators,
- Transistor-based devices (MOSFET, ISFET, etc.),
- Optoelectronics, and
- Coating layers.

It is therefore understandable why AlN thin films have been extensively studied by many research groups over the last couple of years.

The focus of this thesis was the study and improvement of AlN films in view of its application on devices operating at high frequencies. This includes, for instance, sensors, biosensors, filters and oscillators. To this end, the investigation was driven by the improvement of AlN films in different aspects, such as its c-axis orientation, piezoelectric and electroacoustic properties.

The major findings and contributions of this work are summarized below:

1. Improvements of the AlN films properties by doping with Sc. The electromechanical coupling k_t^2 have shown a two fold increase for 15% of Sc concentration (Paper IV).
2. First work to present an experimental characterization of $Al_{(1-x)}Sc_xN$ films as a function of the Sc concentration (electrical and acoustic properties). The optimal Sc concentration (9%) was demonstrated by means of Figure-of-Merit calculations (Paper IV).
3. Deposition of c-axis textured AlN films by HiPIMS directly on Si, at reduced temperatures and in a system with large target-to-substrate distance (Paper I).
4. Sputtering of c-axis tilted films with well-defined thickness and tilt uniformity. The method includes a proposed experimental setup and deposition conditions (Paper V).
5. Design, fabrication and experimental characterization of a device that possesses both properties of voltage transformer and bandpass filter (transfilter) (Paper II).

6. It was demonstrated the possibility to use AlN films as the gate dielectric (high-k material) by means of the fabrication and characterization of MISFET and EISFET devices (Paper III).

My personal opinion about the use of AlN films on devices operating at high frequencies is that the material is close to reach its limits. Certainly the performance of these devices can be improved by changes in the design (electrodes, interdigital transducers, and so on). However, in terms of materials, AlN films may not be substantially improved. The conditions to obtain highly c-axis oriented and tilted films (for application in sensors operating in viscous media, for instance) are well-known and deeply studied. Significant enhancements can most certainly not be achieved from pure AlN films. However, by doping the AlN films with metalloids and transition metals this scenario can be changed. Thus, improvements in the piezoelectric properties of AlN films by means of film doping have received strong attention over the last years. This thesis used Sc as a dopant, and the results confirm that $Al_{(1-x)}Sc_xN$ films are promising, which has been confirmed by other studies as well. I believe that a new range of possibilities is open by doping AlN films.

Resumo em Português

Uma tradução aproximada do título desta tese seria “Síntese de filmes finos de AlN piezoelétrico para aplicações em sensores e dispositivos de alta frequência”.

O termo “dispositivos de alta frequência” é amplo, mas neste trabalho refere-se a dispositivos utilizados em telecomunicações e transmissão de dados, como telefones celulares e redes WLAN (wireless local area network, ou rede local sem fio).

É perceptível o grande avanço que dessas tecnologias nos últimos anos. Como exemplo dos telefones celulares modernos (ou smartphones), estes dispositivos são utilizados nos dias atuais não apenas para transmissão de voz, mas também para transmissão de dados (fotos, vídeos, e-mails, etc.). Em relação às redes locais sem fio, sua utilização se expande cada vez mais. Atualmente é possível conectar-se à rede mundial de computadores (internet) sem utilizar cabos, conectores ou qualquer outra forma física de conexão em ambientes residencias, empresarias e de entretenimento.

Todos estes dispositivos requerem a utilização de componentes como osciladores e filtros de frequência. E para atender o avanço das tecnologias citadas anteriormente, os requisitos de fabricação e funcionamento destes componentes são cada vez mais altos. Redução das dimensões físicas e custo de fabricação são alguns destes requisitos, o que requer o desenvolvimento de novos dispositivos para atender os atuais requisitos. Neste sentido, a utilização de filmes finos associada a dispositivos eletroacústicos tem sido amplamente utilizada em dispositivos de alta frequência. O termo dispositivo eletroacústicos refere-se a dispositivos que se utilizam das propriedades inerentes dos materiais piezoelétricos que os compõem para converter energia mecânica em energia elétrica (e vice-versa). Uma grande vantagem em associar filmes finos a dispositivos eletroacústicos é a possibilidade de integração com a tecnologia de circuitos integrados.

Porém, a utilização de dispositivos eletroacústicos é muito mais ampla do que apenas a filtros e osciladores. É cada vez mais comum a aplicação destes dispositivos como sensores, pois uma variação na frequência de ressonância pode ser diretamente relacionada a variações na grandeza medida (massa, pressão, temperatura, fluxo, etc.). Enfatizando o conceito, a variação da grandeza medida provoca uma variação física no material piezoelétrico através do qual a onda acústica se propaga. Consequentemente, uma variação física na estrutura da camada piezoelétrica é refletida na onda

acústica que se propaga nesta camada (mudança da frequência de ressonância).

Importante observar que a qualidade da camada piezoelétrica dos dispositivos eletroacústicos é crucial para definir a performance dos mesmos. Redução de perdas acústicas e alargamento da faixa de operação são algumas das características que são melhoradas como consequência da melhoria na qualidade da camada piezoelétrica. Estas melhorias incluem, por exemplo, aumento do coeficiente de acoplamento eletromagnético (k_t^2). Este coeficiente indica a eficiência do material piezoelétrico em converter energia elétrica em mecânica (acústica), e vice-versa. Vários estudos na literatura científica comprovam que quanto melhor a textura do filme piezoelétrico, maior o valor de k_t^2. Entenda-se por melhor textura da camada piezoelétrica quando o material tem sua estrutura orientada perpendicularmente à superfície.

Porém, ao utilizar dispositivos eletroacústicos como sensores, algumas aplicações requerem filmes piezoelétricos inclinados, ou seja, filmes com estrutura não perpendicular à superfície. Mais especificamente, sensores utilizados em meio líquido/viscoso. Isto se deve ao fato de que as perdas das ondas acústicas para o meio líquido são reduzidas ao se utilizar filmes piezoelétricos com estrutura inclinada.

Este trabalho utilizou Nitreto de Alumínio (AlN) como material piezoelétrico de estudo. Decerto que existem outros materiais piezoelétricos com boas propriedades, alguns inclusive com características pontuais melhores que o AlN. O que torna o AlN um material de grande interesse é a combinação de boas propriedades em um único elemento. Alta velocidade de propagação acústica, baixa perda acústica, alta resistividade elétrica, alta condutividade térmica e larga banda de energia são algumas dessas características. Além disso, AlN é quimicamente estável e totalmente compatível com a tecnologia de fabricação de circuitos integrados.

É necessário observar que há um constante interesse no desenvolvimento de novos materiais piezoelétricos que, assim como o AlN, reúnam boas propriedades em um único elemento. Isso permitirá a fabricação de dispositivos eletroacústicos com melhor desempenho. Muitos estudos recentes têm demonstrado o beneficial efeito nas propriedades piezoelétricas quando materiais dopantes como Escândio (Sc), Boro (B) e Ítrio (Y) (entre outros) são adicionados a filmes de AlN.

Nesse contexto, algumas das principais contribuições desta tese são listadas a seguir:

1. Dopagem e caracterização experimental de filmes de AlN em função da concentração de Sc são apresentadas no Artigo IV. Os filmes de AlN foram dopados até a concentração máxima de 15% de Sc e os resultados indicam um aumento de 100% no coeficiente k_t^2 para esta concentração máxima. Estes filmes são denominados AlScN (Nitreto de Alumínio Escândio).

2. No Artigo V é apresentado um processo de deposição que permite a obtenção de filmes de AlN inclinados e com boa uniformidade de espessura e inclinação do filme sobre a área depositada (substrato de Silício). Este processo inclui a utilização de uma matriz de alvos de Al inclinados em combinação com condições de deposição específicas.
3. Deposição de filmes de AlN com boa textura diretamente sobre substratos de Si, a temperaturas reduzidas e em um sistema com grande distância alvo-substrato (Artigo I). A técnica de deposição utilizada é denominada HiPIMS (high power impulse magnetron sputtering, ou pulverização catódica por impulso de alta potência). As três condições listadas anteriormente (substrato de Si, reduzida temperatura e grande distância entre alvo e substrato) não são as mais propícias ao crescimento de filmes orientados. A técnica de deposição utilizada transmite maior energia aos íons, o que por consequência e favorável ao crescimento desses filmes. Os resultados indicam que é possível obter filmes de AlN com boa qualidade e depositados a temperaturas reduzidas ao utilizar-se a técnica HiPIMS.

Sammanfattning på Svenska

En ungefärlig översättning av titeln på denna avhandling är "Syntes av tunna piezoelektriska AlN filmer för sensorer och högfrekvensanordningar".

Termen "högfrekvensanordningar" är bred men avser i detta arbete anordningar som används inom telekom och dataöverföring, till exempel i mobiltelefoner och WLAN (trådlösa lokala nätverk).

Det har skett anmärkningsvärda förbättringar inom dessa tekniker de senaste åren. Ett exempel är moderna mobiltelefoner (eller smartphones). Dessa enheter används numera inte bara för röst, utan även för dataöverföring (foton, videor, e-post etc.). Beträffande trådlösa lokala nätverk så ökar deras användning mer och mer och det är numera möjligt att ansluta till webben (internet) utan kablar, kontakter eller någon annan form av fysisk anslutning i bostäder, företag och miljöer för nöjen.

Alla dessa anordningar kräver komponenter såsom oscillatorer och frekvensfilter. För att möta efterfrågan på tidigare nämnda tekniker blir kraven på tillverkning och drift av dessa komponenter allt högre. Minskade tillverkningskostnader och fysiska dimensioner är några av kraven som driver på utvecklingen av nya anordningar för att möta dagens behov. I detta avseende har användningen av tunna filmer förknippade med elektroakustiska anordningar använts i stor utsträckning i högfrekvensanordningar. Termen elektroakustisk enhet avser anordningar som använder de inneboende egenskaperna hos de piezoelektriska material som de är tillverkade av (omvandling av mekanisk till elektrisk energi, och vice versa). En distinkt fördel med de tunnfilmsbaserade elektroakustiska anordningarna är möjligheten att integrera dem med tekniken för integrerade kretsar.

Dock är användningsområdet av elektroakustiska anordningar mycket större än bara i filter och oscillatorer. Det blir allt vanligare att använda sådana anordningar som sensorer eftersom en förändring av resonansfrekvensen kan vara direkt relaterad till variationer av den uppmätta kvantiteten (massa, tryck, temperatur, flöde, etc.). För att förtydliga konceptet; variationen i den uppmätta kvantiteten orsakar en fysisk förändring i det piezoelektriska materialet genom vilket den akustiska vågen fortplantar sig. Följaktligen återspeglas en variation av den fysiska strukturen hos det piezoelektriska skiktet i den akustiska våg som utbreder sig i detta skikt (förändring av resonansfrekvensen).

Det bör noteras att kvaliteten på det piezoelektriska skiktet i de elektroakustiska anordningarna är avgörande för deras prestanda. Minskade akustiska förluster och bredare bandpassfrekvens är några av de egenskaper som förbättras genom att höja kvaliteten på det piezoelektriska skiktet. Dessa förbättringar innefattar exempelvis att öka den magnetiska kopplingskoefficienten (k_t^2). Denna koefficient indikerar verkningsgraden hos det piezoelektriska materialet att omvandla elektrisk till mekanisk energi (akustisk), och vice versa. Flera studier i litteraturen visar att ju bättre textur på det piezoelektriska skiktet, desto större värde på k_t^2. Med uttrycket ”bättre textur på det piezoelektriska skiktet” menas när materialet har en struktur vinkelrätt orienterat mot ytan.

Dock kräver vissa applikationer lutande piezoelektriska filmer (dvs filmer med icke-vinkelrät struktur) vid bruk av elektroakustiska anordningar som sensorer. Mer specifikt, sensorer som är verksamma i vätska/visköst medium. Detta beror på det faktum att förlusterna av akustiska vågor till det flytande mediet är mindre för piezoelektriska filmer med lutande struktur.

Denna avhandling använde Aluminiumnitrid (AlN) som det studerade piezoelektriska materialet. Förvisso finns det andra piezoelektriska material med goda egenskaper. Emellertid är AlN ett material av stort intresse grund av en kombination av flera goda egenskaper i ett och samma material. Hög akustisk utbredningshastighet, låga akustiska förluster, hög elektrisk resistivitet, hög värmeledningsförmåga och stort bandgap är några av dessa egenskaper. Dessutom är AlN kemiskt stabilt och helt kompatibelt med tekniken för integrerade kretsar.

Det bör noteras att det finns ett ökande intresse för att utveckla förbättrade AlN skikt samt nya piezoelektriska material som har alla goda egenskaper i ett och samma material. Detta kommer att möjliggöra tillverkning av elektroakustisk anordningar med bättre prestanda. Flera senare studier har påvisat en gynnsam effekt på de piezoelektriska egenskaperna genom dopning av AlN filmer med material såsom Sc, Y och B.

I detta sammanhang återges några av de viktigaste bidragen från denna avhandling nedan:

1. Dopning och karakterisering av AlN filmer som en funktion av Sc koncentration presenteras i Artikel IV. AlN filmerna dopades upp till en maximal Sc koncentration på 15% och resultaten indikerar en ökning på 100% för kopplingskoefficienten k_t^2 vid denna maximala koncentration. Dessa filmerna är så kallade AlScN (Aluminumskandiumnitrid).
2. I Artikel V presenteras en deponeringsprocess för att få lutande AlN filmer med god uniformitet med avseende på tjocklek och lutning. Denna process innefattar nyttjandet av en uppsättning lutande Al targetar i kombination med specifika processförhållanden.

3. Deponering av AlN filmer med god textur direkt på Si-substrat vid lägre temperaturer och i ett system med ett stort avstånd mellan target och substrat (Artikel I). Deponeringstekniken som används kallas HiPIMS (högeffekt impuls magnetron sputtering). De tre betingelserna som specificerades ovan (Si-substrat, lägre temperatur och stort avstånd mellan target och substrat) inte är de mest gynnsamma för deponering av orienterade filmer. Den använda deponeringstekniken ger mer kinetisk energi till atomerna som bygger upp filmen vilket gynnar tillväxten av orienterade filmer. Resultaten har dock en principiellt viktig betydelse eftersom de visar att man genom detta förfarande kan få bra kvalitet på skikten vid en lägre temperatur om man kompenserar med en högre kinetisk energi på de infallande atomerna. Detta möjliggör beläggning av temperaturkänsliga substrat.

Acknowledgments

It is not unusual that research and PhD studies go through a long and not necessarily straightforward way. So many things can happen… So many things can go wrong. You never know. The only way to figure it out is… GO! And I couldn't have made it to this point if I was alone. So, I would like to express my eternal gratitude to all of you!

PS: I hope I hadn't forgotten anyone. But if this happened, just let me know and we can schedule an "I'm sorry" fika.

(in no specific order)

Ioshiaki Doi, my supervisor in Brazil, for your wise and careful advice. I could always count on you!

Ilia Katardjiev, my supervisor in Sweden, for taking me on as a guest PhD student and letting me continue working in the Thin Films Group after the first year.

J. A. Diniz, always open to hear how things are going, plans for the future... Thank you for your valuable advice and suggestions!

Jair Fernandes, sharing research projects with you was a pleasure.

Johan Bjurström, co-worker and co-supervisor for a while, I learned a lot with you when we worked together.

Jörgen Ohlsson, thank you for standing by my side when necessary. I really appreciated it! And thank you for helping me through the final steps of the PhD studies.

Tomas Nyberg, we worked together for a short period, but your contributions were essential to the improvement of this work.

Tomas Kubart, thank you for the common project and for bringing me to the HiPIMS world.

Örjan Vallin, constantly ready to help (and to understand my “dålig svenska”). And thank you for supporting me when I crashed the MRD-I.

Marianne Asplund, you were an angel for me at FTE. Always taking care of me, checking if everything was alright. Very kind!

Regina and Mara, for the mind refreshing coffee breaks and very nice talks.

To the CCS and MSL staff, for all the help with the clean room work.

Pedro Salomé, you were so patient hearing all my bla-bla-bla! Thank you for your friendship, relaxing fikas and valuable advice.

Sara, Shabnam, Linli, Wiliana, Janaína, Valeria, Johan A., Saman-san, Kiran, Katia, Markus, Juan, Jose, Jessica and Oscar, than you for boosting my days with talks, laughing and nice fika time. Your friendship is invaluable!

Ulf Sahlin, min älskling, thank you for you unwearying support. Always encouraging me, you hold my hand, you make me stronger. Tack, sötnos!

Last but certainly not least, my family. Minha família querida, eu nem sei o que dizer... eu nem sei como agradecer. Palavras não conseguem expressar o sentimento e o significado do quanto eu sou grata a vocês! Constantemente me apoiando, constantemente me incentivando, mesmo que minhas decisões nos afastem fisicamente. De todo coração, com toda força de minha alma, meu muito obrigada! Eu amo vocês!

Milena de Albuquerque Moreira

References

[1] M. Ishihara, S. J. Li, H. Yumoto, K. Akashi, and Y. Ide, "Control of preferential orientation of AlN films prepared by the reactive sputtering method," *Thin Solid Films,* vol. 316, pp. 152-157, 1998.

[2] F. Engelmark, G. F. Iriarte, I. V. Katardjiev, M. Ottosson, P. Muralt, and S. Berg, "Structural and electroacoustic studies of AlN thin films during low temperature radio frequency sputter deposition," *Journal of Vacuum Science & Technology A,* vol. 19, pp. 2664-2669, 2001.

[3] X.-H. Xu, H.-S. Wu, C.-J. Zhang, and Z.-H. Jin, "Morphological properties of AlN piezoelectric thin films deposited by DC reactive magnetron sputtering," *Thin Solid Films,* vol. 388, pp. 62-67, 2001.

[4] F. Engelmark, J. Westlinder, G. F. Iriarte, I. V. Katardjiev, and J. Olsson, "Electrical Characterization of AlN MIS and MIM Structures," *IEEE Transactions on Electron Devices,* vol. 50, pp. 1214-1219, 2003.

[5] A. Fathimulla and A. A. Lakhani, "Reactively rf magnetron sputtered AlN films as gate dielectric," *Journal of Applied Physics,* vol. 54, pp. 4586-4589, 1983.

[6] G. F. Iriarte, J. G. Rodríguez, and F. Calle, "Synthesis of c-axis oriented AlN thin films on different substrates: A review," *Materials Research Bulletin,* vol. 45, pp. 1039-1045, 2010.

[7] G. Wingqvist, F. Tasnadi, A. Zukauskaite, J. Birch, H. Arwin, and L. Hultman, "Increased electromechanical coupling in w-$Sc_xAl_{(1-x)}N$," *Applied Physics Letters,* vol. 97, 2010.

[8] S.-T. Lee, B.-G. Park, M.-D. Kim, J.-E. Oh, S.-G. Kim, Y.-H. Kim*, et al.*, "Control of polarity and defects in the growth of AlN films on Si (111) surfaces by inserting an Al interlayer," *Current Applied Physics,* vol. 12, pp. 385-388, 2012.

[9] B. Liu, J. Gao, K. M. Wu, and C. Liu, "Preparation and rapid thermal annealing of AlN thin films grown by molecular beam epitaxy," *Solid State Communications,* vol. 149, pp. 715-717, 2009.

[10] M.-J. Lai, L.-B. Chang, T.-T. Yuan, and R.-M. Lin, "Improvement of crystal quality of AlN grown on sapphire substrate by MOCVD," *Crystal Research and Technology,* vol. 45, pp. 703-706, 2010.

[11] J.-W. Soh, S.-S. Jang, I.-S. Jeong, and W.-J. Lee, "C-axis orientation of AlN films prepared by ECR PECVD," *Thin Solid Films,* vol. 279, pp. 17-22, 1996.

[12] C.-M. Yang, K. Uehara, S.-K. Kim, S. Kameda, H. Nakase, and K. Tsubouchi, "Highly c-axis-oriented AlN film using MOCVD for 5GHz-band FBAR filter," in *IEEE International Ultrasonics Symposium Proceedings*, 2003, pp. 170-173.

[13] M. Clement, E. Iborra, J. Sangrador, A. Sanz-Hervás, L. Vergara, and M. Aguilar, "Influence of sputtering mechanisms on the preferred orientation of aluminum nitride thin films," *Journal of Applied Physics,* vol. 94, pp. 1495-1500, 2003.

[14] T. Kumada, M. Ohtsuka, K. Takada, and H. Fukuyama, "Influence of sputter power and N_2 gas flow ratio on crystalline quality of AlN layers deposited at 823 K by RF reactive sputtering," *Physica Status Solidi (c),* vol. 9, pp. 515-518, 2012.
[15] Y. Z. You and D. Kim, "Influence of incidence angle and distance on the structure of aluminium nitride films prepared by reactive magnetron sputtering," *Thin Solid Films,* vol. 515, pp. 2860-2863, 2007.
[16] K. A. Aissa, A. Achour, J. Camus, L. L. Brizoual, P.-Y. Jouan, and M.-A. Djouadi, "Comparison of the structural properties and residual stress of AlN films deposited by dc magnetron sputtering and high power impulse magnetron sputtering at different working pressures," *Thin Solid Films,* vol. 550, pp. 264-267, 2013.
[17] A. Guillaumot, F. Lapostolle, C. Dublanche-Tixier, J. C. Oliveira, A. Billard, and C. Langlade, "Reactive deposition of Al–N coatings in Ar/N_2 atmospheres using pulsed-DC or high power impulse magnetron sputtering discharges," *Vacuum,* vol. 85, pp. 120-125, 2010.
[18] K. Kusaka, D. Taniguchi, T. Hanabusa, and K. Tominaga, "Effect of sputtering gas pressure and nitrogen concentration on crystal orientation and residual stress in sputtered AlN films," *Vacuum,* vol. 66, pp. 441-446, 2002.
[19] K.-H. Chiu, H.-R. Chen, and S. R.-S. Huang, "High-Performance Film Bulk Acoustic Wave Pressure and Temperature Sensors," *Japanese Journal of Applied Physics,* vol. 46, pp. 1392-1397, 2007.
[20] A. Choujaa, N. Tirole, C. Bonjour, G. Martin, D. Hauden, P. Blind*, et al.*, "AlN/silicon Lamb-wave microsensors for pressure and gravimetric measurements," *Sensors and Actuators A: Physical,* vol. 46, pp. 179-182, 1995.
[21] L. Zhou, J.-F. Manceau, and F. Bastien, "Interaction between gas flow and a Lamb waves based microsensor," *Sensors and Actuators A: Physical,* vol. 181, pp. 1-5, 2012.
[22] R. Gabl, E. Green, M. Schreiter, H. D. Feucht, H. Zeininger, R. Primig*, et al.*, "Novel integrated FBAR sensors: a universal technology platform for bio- and gas-detection," in *IEEE Sensors*, 2003, pp. 1184-1188.
[23] G. Wingqvist, "AlN-based sputter-deposited shear mode thin film bulk acoustic resonator (FBAR) for biosensor applications — A review," *Surface and Coatings Technology,* vol. 205, pp. 1279-1286, 2010.
[24] M. Nirschl, A. Blüher, C. Erler, B. Katzschner, I. Vikholm-Lundin, S. Auer*, et al.*, "Film bulk acoustic resonators for DNA and protein detection and investigation of in vitro bacterial S-layer formation," *Sensors and Actuators A: Physical,* vol. 156, pp. 180-184, 2009.
[25] I. Katardjiev and V. Yantchev, "Recent developments in thin film electro-acoustic technology for biosensor applications," *Vacuum,* vol. 86, pp. 520-531, 2012.
[26] L. Liljeholm, M. Junaid, T. Kubart, J. Birch, L. Hultman, and I. Katardjiev, "Synthesis and characterization of (0001)-textured wurtzite $Al_{(1-x)}B_xN$ thin films," *Surface and Coatings Technology,* vol. 206, pp. 1033-1036, 2011.
[27] L. Liljeholm and J. Olsson, "Electrical characterization of wurtzite (Al,B)N thin films," *Vacuum,* vol. 86, pp. 466-470, 2011.
[28] J.-H. Song, J.-L. Huang, T. Omori, J. C. Sung, S. Wu, H.-H. Lu*, et al.*, "Growth of highly c-axis oriented (B, Al)N film on diamond for high frequency surface acoustic wave devices," *Thin Solid Films,* vol. 520, pp. 2247-2250, 2012.
[29] E. Iborra, J. Capilla, J. Olivares, M. Clement, and V. Felmetsger, "Piezoelectric and electroacoustic properties of Ti-doped AlN thin films as a function of Ti

content," in *IEEE International Ultrasonics Symposium*, Dresden, 2012, pp. 2734 - 2737.
[30] M. Akiyama, T. Kamohara, K. Kano, A. Teshigahara, Y. Takeuchi, and N. Kawahara, "Enhancement of Piezoelectric Response in Scandium Aluminum Nitride Alloy Thin Films Prepared by Dual Reactive Cosputtering," *Advanced Materials,* vol. 21, pp. 593-597, 2009.
[31] A. Teshigahara, K.-Y. Hashimoto, and M. Akiyama, "Scandium aluminum nitride: Highly piezoelectric thin film for RF SAW devices in multi GHz range " in *IEEE International Ultrasonics Symposium*, Dresden, 2012, pp. 1-5.
[32] A. Žukauskaitė, C. Tholander, J. Palisaitis, P. O. Å. Persson, V. Darakchieva, N. B. Sedrine*, et al.*, "$Y_xAl_{(1-x)}N$ thin films," *Journal of Physics D: Applied Physics,* vol. 45, p. 422001, 2012.
[33] J. T. Luo, B. Fan, F. Zeng, and F. Pan, "Influence of Cr-doping on microstructure and piezoelectric response of AlN films," *Journal of Physics D: Applied Physics,* vol. 42, p. 235406, 2009.
[34] V. V. Felmetsger and M. K. Mikhov, "Reactive Magnetron Sputtering of Piezoelectric Cr-Doped AlN Thin Films," in *IEEE Ultrasonic Symposium 2011*, 2011, pp. 835-839.
[35] H. Liu, F. Zeng, G. Tang, and F. Pan, "Enhancement of piezoelectric response of diluted Ta doped AlN," *Applied Surface Science,* vol. 270, pp. 225-230, 2013.
[36] E. Iborra, J. Olivares, M. Clement, L. Vergara, A. Sanz-Hervás, and J. Sangrador, "Piezoelectric properties and residual stress of sputtered AlN thin films for MEMS applications," *Sensors and Actuators A: Physical,* vol. 115, pp. 501-507, 2004.
[37] Erik Särhammar, Erik Strandberg, Nicolas Martin, and T. Nyberg, "Sputter Rate Distribution and Compositional Variations in Films Sputtered from Elemental and Multi-Element Targets at Different Pressures," *International Journal of Materials Science and Applications,* vol. 3, pp. 29-36, 2014.
[38] G. F. Iriarte, F. Engelmark, and I. V. Katardjiev, "Reactive Sputter Deposition of Highly Oriented AlN Films at Room Temperature," *Journal of Materials Research,* vol. 17, pp. 1469-1475, 2002.
[39] G. F. Iriarte, J. Bjurstrom, J. Westlinder, F. Engelmark, and I. V. Katardjiev, "Synthesis of c-axis-oriented AlN thin films on high-conducting layers: Al, Mo, Ti, TiN, and Ni," *IEEE Transactions on Ultrasonics, Ferroelectrics and Frequency Control,* vol. 52, pp. 1170-1174, 2005.
[40] J. Bjurström, G. Wingqvist, and I. Katardjiev, "Synthesis of Textured Thin Piezoelectric AlN Films With a Nonzero C-Axis Mean Tilt for the Fabrication of Shear Mode Resonators," *IEEE Transactions on Ultrasonics Ferroelectrics and Frequency Control,* vol. 53, pp. 2095-2100, 2006.
[41] Y.-C. Chen, W.-T. Chang, K.-S. Kao, C.-H. Yang, and C.-C. Cheng, "The Liquid Sensor Using Thin Film Bulk Acoustic Resonator with C-Axis Tilted AlN Films," *Journal of Nanomaterials,* vol. 2013, p. 8, 2013.
[42] J. Xiong, H.-S. Gu, W. Wu, M.-Z. Hu, P.-F. Du, and H. Xie, "Synthesis of c-Axis Inclined AlN Films in an Off-Center System for Shear Wave Devices," *Journal of Electronic Materials,* vol. 40, pp. 1578-1583, 2011.
[43] R. Deng, P. Muralt, and D. Gall, "Biaxial texture development in aluminum nitride layers during off-axis sputter deposition," *Journal of Vacuum Science & Technology A,* vol. 30, pp. 051501-1 - 051501-9, 2012.
[44] F. Martin, M. E. Jan, S. Rey-Mermet, B. Belgacem, D. Su, M. Cantoni*, et al.*, "Shear mode coupling and tilted grain growth of AlN thin films in BAW

resonators," *Ultrasonics, Ferroelectrics and Frequency Control, IEEE Transactions on,* vol. 53, pp. 1339-1343, 2006.
[45] A. A. Turkin, Y. T. Pei, K. P. Shaha, C. Q. Chen, D. I. Vainshtein, and J. T. M. De Hosson, "On the evolution of film roughness during magnetron sputtering deposition," *Journal of Applied Physics,* vol. 108, pp. 094330-094330-9, 2010.
[46] D. Deniz, J. M. E. Harper, J. W. Hoehn, and F. Chen, "Tilted fiber texture in aluminum nitride thin films," *Journal of Vacuum Science & Technology A,* vol. 25, pp. 1214-1218, 2007.
[47] N. S. Dellas and J. M. E. Harper, "Effect of deposition angle on fiber axis tilt in sputtered aluminum nitride and pure metal films," *Thin Solid Films,* vol. 515, pp. 1647-1650, 2006.
[48] T. Karabacak, "Thin-film growth dynamics with shadowing and re-emission effects," *Journal of Nanophotonics,* vol. 5, pp. 052501-052501-18, 2011.
[49] P. Stempflé, A. Besnard, N. Martin, A. Domatti, and J. Takadoum, "Accurate control of friction with nanosculptured thin coatings: Application to gripping in microscale assembly," *Tribology International,* vol. 59, pp. 67-78, 2013.
[50] G. Wingqvist, "Thin-film electro-acoustic sensors based on AlN and its alloys: possibilities and limitations," *Microsystem Technologies,* vol. 18, pp. 1213-1223, 2012.
[51] J.-C. Yang, X.-Q. Meng, C.-T. Yang, and Y. Zhang, "Influence of sputtering power on crystal quality and electrical properties of Sc-doped AlN film prepared by DC magnetron sputtering," *Applied Surface Science,* vol. 287, pp. 355-358, 2013.
[52] M. Akiyama, K. Kano, and A. Teshigahara, "Influence of growth temperature and scandium concentration on piezoelectric response of scandium aluminum nitride alloy thin films," *Applied Physics Letters,* vol. 95, pp. 162107-162107-3, 2009.
[53] F. Tasnadi, B. Alling, C. Hoglund, G. Wingqvist, J. Birch, L. Hultman*, et al.*, "Origin of the Anomalous Piezoelectric Response in Wurtzite $Sc_xAl_{1-x}N$ Alloys," *Physical Review Letters,* vol. 104, pp. 137601-1 - 137601-4, 2010.
[54] A. A. Vives, *Piezoelectric Transducers and Applications*: Springer, 2008.
[55] D. Eom, S. Y. No, C. S. Hwang, and H. J. Kim, "Properties of Aluminum Nitride Thin Films Deposited by an Alternate Injection of Trimethylaluminum and Ammonia under Ultraviolet Radiation," *Journal of The Electrochemical Society,* vol. 153, pp. C229-C234, 2006.
[56] E. P. Gusev, D. A. Buchanan, E. Cartier, A. Kumar, D. DiMaria, S. Guha*, et al.*, "Ultrathin high-K gate stacks for advanced CMOS devices," in *Electron Devices Meeting, 2001. IEDM '01. Technical Digest. International*, 2001, pp. 20.1.1-20.1.4.
[57] K. Sarakinos, J. Alami, and S. Konstantinidis, "High power pulsed magnetron sputtering: A review on scientific and engineering state of the art," *Surface and Coatings Technology,* vol. 204, pp. 1661-1684, 2010.
[58] U. Helmersson, M. Lattemann, J. Bohlmark, A. P. Ehiasarian, and J. T. Gudmundsson, "Ionized physical vapor deposition (IPVD): A review of technology and applications," *Thin Solid Films,* vol. 513, pp. 1-24, 2006.
[59] J. Böhlmark, "Fundamentals of high power impulse magnetron sputtering," 2006.
[60] J. T. Gudmundsson, "Ionized physical vapor deposition (IPVD): magnetron sputtering discharges," *Journal of Physics: Conference Series,* vol. 100, p. 082002, 2008.

[61] J. T. Gudmundsson, N. Brenning, D. Lundin, and U. Helmersson, "High power impulse magnetron sputtering discharge," *Journal of Vacuum Science & Technology A,* vol. 30, pp. -, 2012.
[62] H. Jin, B. Feng, S. Dong, C. Zhou, J. Zhou, Y. Yang*, et al.*, "Influence of Substrate Temperature on Structural Properties and Deposition Rate of AlN Thin Film Deposited by Reactive Magnetron Sputtering," *Journal of Electronic Materials,* vol. 41, pp. 1948-1954, 2012.
[63] A. Artieda, M. Barbieri, C. S. Sandu, and P. Muralt, "Effect of substrate roughness on c-oriented AlN thin films," *Journal of Applied Physics,* vol. 105, pp. 024504-024504-6, 2009.
[64] T. Kamohara, M. Akiyama, N. Uena, and N. Kuwano, "Improvement in crystal orientation of AlN thin films prepared on Mo electrodes using AlN interlayers," *Ceramics International,* vol. 34, pp. 985-989, 2008.
[65] T. Kamohara, M. Akiyama, N. Ueno, K. Nonaka, and H. Tateyama, "Growth of highly c-axis-oriented aluminum nitride thin films on molybdenum electrodes using aluminum nitride interlayers," *Journal of Crystal Growth,* vol. 275, pp. 383-388, 2005.
[66] H. Y. Liu, G. S. Tang, F. Zeng, and F. Pan, "Influence of sputtering parameters on structures and residual stress of AlN films deposited by DC reactive magnetron sputtering at room temperature," *Journal of Crystal Growth,* vol. 363, pp. 80-85, 2013.
[67] C.-M. Lin, T.-T. Yen, V. V. Felmetsger, M. A. Hopcroft, J. H. Kuypers, and A. P. Pisano, "Thermally compensated aluminum nitride Lamb wave resonators for high temperature applications," *Applied Physics Letters,* vol. 97, pp. 083501-1 - 083501-3, 2010.
[68] G. Wingqvist, L. Arapan, V. Yantchev, and I. Katardjiev, "A micromachined thermally compensated thin film Lamb wave resonator for frequency control and sensing applications," *Journal of Micromechanics and Microengineering,* vol. 19, p. 035018, 2009.
[69] J. H. Kuypers, L. Chih-Ming, G. Vigevani, and A. P. Pisano, "Intrinsic temperature compensation of aluminum nitride Lamb wave resonators for multiple-frequency references," in *Frequency Control Symposium, 2008 IEEE International*, 2008, pp. 240-249.
[70] Ahmad Safari and E. K. Akdoğan, *Piezoelectric and Acoustic Materials for Transducer Applications*: Springer, 2008.
[71] S. Trolier-McKinstry and P. Muralt, "Thin Film Piezoelectrics for MEMS," *Journal of Electroceramics,* vol. 12, pp. 7-17, 2004.

Acta Universitatis Upsaliensis

Digital Comprehensive Summaries of Uppsala Dissertations from the Faculty of Science and Technology 1160

Editor: The Dean of the Faculty of Science and Technology

A doctoral dissertation from the Faculty of Science and Technology, Uppsala University, is usually a summary of a number of papers. A few copies of the complete dissertation are kept at major Swedish research libraries, while the summary alone is distributed internationally through the series Digital Comprehensive Summaries of Uppsala Dissertations from the Faculty of Science and Technology. (Prior to January, 2005, the series was published under the title "Comprehensive Summaries of Uppsala Dissertations from the Faculty of Science and Technology".)

Distribution: publications.uu.se
urn:nbn:se:uu:diva-229588

ACTA
UNIVERSITATIS
UPSALIENSIS
UPPSALA
2014